TOR Complex 2-regulated protein kinase Fpk1 stimulates endocytosis via inhibition of Ark1/Prk1-related protein kinase Akl1 in *Saccharomyces cerevisiae*

Françoise M. Roelants, Kristin L. Leskoske, Ross T.A. Pedersen,

Alexander Muir[1], Jeffrey M.-H. Liu[2], Gregory C. Finnigan[3] and Jeremy Thorner*

Divisions of Biochemistry, Biophysics & Structural Biology and Cell & Developmental Biology,

Department of Molecular and Cell Biology,

University of California, Berkeley, CA 94720-3202 USA

Running head: Protein kinase Fpk1 inhibits endocytic protein kinase Akl1

[1]Current address: Dept. of Biology and Koch Institute for Integrative Cancer Research, Massachusetts Institute of Technology, Cambridge, MA.

[2]Current address: Dept. of Biological Engineering, Univ. of Michigan, Ann Arbor, MI.

[3]Current address: Dept. of Biochemistry and Molecular Biophysics, Kansas State Univ., Manhattan, KS.

*To whom correspondence should be addressed:
Professor Jeremy Thorner
Division of Biochemistry, Biophysics and Structural Biology
Department of Molecular and Cell Biology
University of California at Berkeley
Room 16, Barker Hall
Berkeley, CA 94720-3202 USA
Phone: (510) 642-2558
FAX: (510) 642-6420
e-mail: jthorner@berkeley.edu

ABSTRACT

Depending on the stress, plasma membrane alterations activate or inhibit yeast Target of Rapamycin (TOR) Complex 2, which, in turn, upregulates or downregulates the activity of its essential downstream effector, protein kinase Ypk1. Through phosphorylation of multiple substrates, Ypk1 controls many processes that restore homeostasis. One such substrate is protein kinase Fpk1, which is negatively regulated by Ypk1. Fpk1 phosphorylates and stimulates flippases that translocate aminoglycerophospholipids from the outer to the inner leaflet of the plasma membrane. Fpk1 has additional roles, but other substrates were uncharacterized. We show that Fpk1 phosphorylates and inhibits protein kinase Akl1, related to protein kinases Ark1 and Prk1 that modulate the dynamics of actin patch-mediated endocytosis. Akl1 has two Fpk1 phosphorylation sites (Ark1 and Prk1 have none) and is hypophosphorylated when Fpk1 is absent. Conversely, under conditions that inactivate TORC2-Ypk1 signaling, which alleviates Fpk1 inhibition, Akl1 is hyperphosphorylated. Monitoring phosphorylation of known Akl1 substrates (Sla1 and Ent2) confirmed that Akl1 is hyperactive when not phosphorylated by Fpk1. Fpk1-mediated negative regulation of Akl1 enhances endocytosis because an Akl1 mutant immune to Fpk1 phosphorylation causes faster dissociation of Sla1 from actin patches, confers elevated resistance to doxorubicin (a toxic compound whose entry requires endocytosis), and impedes lucifer yellow uptake (a marker of fluid phase endocytosis). Thus, TORC2-Ypk1, by regulating Fpk1-mediated phosphorylation of Akl1, adjusts the rate of endocytosis.

INTRODUCTION

Plasma membrane (PM) function requires continual adjustment of its protein and lipid content and distribution. Critical processes, such as exocytosis (1), endocytosis (2) and signaling by ligand-sensing receptors (3), are dramatically impaired if PM constitution is altered. Conversely, the same processes that rely on maintenance of proper PM structure also remodel the PM by eliciting responses that alter the protein and lipid species present (4,5). Thus, cells must have mechanisms to sense the status of the PM and effector pathways that modulate the reactions needed to maintain homeostasis and preserve the functional state of the PM in the face of changing circumstances and stimuli.

Studies in budding yeast (*Saccharomyces cerevisiae*) have revealed that the PM-associated Target of Rapamycin (TOR) Complex 2 (TORC2) serves as both a sensor and regulator of PM status. TORC2 activity is stimulated by certain stresses that perturb the PM, including inhibition of sphingolipid synthesis (6-8), hypotonic conditions (7,9) and heat shock (10), and is inactivated by other PM perturbing stresses, such as hypertonic conditions (11,12). Although TORC2 seems to 'sense' PM structure, how it does so is unclear. It is thought (7,9) that the membrane stretch evoked by hypotonic shock activates TORC2 by allowing its association with two ancillary subunits (Slm1 and Slm2) (13-15) normally sequestered within a PM domain, dubbed eisosomes (16), distinct from that harboring TORC2. However, the molecular feature(s) sensed by TORC2 upon this or any other PM perturbation, and the ensuing molecular mechanism by which TORC2 activity is affected in each case, are not fully understood.

Better characterized is how TORC2 controls its sole essential downstream effectors, the protein kinase Ypk1 and its paralog Ypk2/Ykr2 (17-20). Focusing on Ypk1, its basal function requires phosphorylation of T504 in its activation loop by the upstream, eisosome-associated protein kinases Pkh1 and Pkh2 (18,21-23). Activating PM stresses promote TORC2-mediated phosphorylation of Ypk1 at additional, C-terminal sites, most prominently S644 and T662, which markedly enhance Ypk1 catalytic activity (6,22); conversely, loss of the modifications installed

by TORC2 dramatically dampens Ypk1 activity (11,12). Strikingly, the lethality arising from the absence of TORC2 activity (24,25) can be rescued by alleles of Ypk1 (or Ypk2) that bypass the need for their TORC2-mediated phosphorylation (6,19), indicating that the sole function of TORC2 essential for cell viability is activation of Ypk1 (or Ypk2). Because *YPK1 ypk2*Δ cells are viable and exhibit no overt phenotype, Ypk1 is an effector that can execute all the essential functions of TORC2. Thus, subsequent characterization of the substrates of Ypk1 has shed considerable light on those precincts of cellular physiology that are under the control of the TORC2-Ypk1 signaling axis.

Indeed, elucidation of Ypk1 targets has demonstrated that it is the primary regulator of PM homeostasis. Ypk1 phosphorylates and negatively regulates endocytic adaptors, like Rod1 and Aly2 (8,26), which promote internalization of nutrient permeases and other classes of integral PM proteins, thereby modulating the protein species in the PM. Ypk1 also phosphorylates and negatively regulates Orm1 and Orm2 (6), which are ER-localized tetraspanins that inhibit the first enzyme unique to sphingolipid biosynthesis (27), thereby increasing flux into this metabolic pathway. In addition, Ypk1 phosphorylates and stimulates ceramide synthase (8), thereby ensuring that pathway up-regulation results in efficient production of its complex sphingolipid end products. In addition, Ypk1 phosphorylates and negatively regulates Gpd1 (11), one of two enzymes that convert DHAP into glycerol-3P (an essential precursor to all glycerophospho-lipids), as well as phosphorylates and opens the Fps1 glyceroaquaporin that controls glycerol efflux (12), further contributing to control of the supply of this building block for PM glycerophospholipids. Moreover, Ypk1 phosphorylates and negatively regulates Fpk1 and its paralog Fpk2/Kin82 (23), protein kinases responsible, in turn, for phosphorylating and activating Dnf1, Dnf2 and Dnf3 (28), three PM-associated P-type ATPases (flippases) that translocate PM aminoglycerophospholipids from the outer to the inner leaflet (29,30), thereby influencing the relative content of these lipid species on the two different sides of the PM bilayer. Thus, TORC2-Ypk1 signaling regulates multiple factors that influence the protein and lipid

105 composition, as well as lipid distribution, in the PM.

106 In addition to its negative regulation by Ypk1-mediated phosphorylation in response to those
107 PM stresses that activate TORC2, Fpk1 is also phosphorylated and negatively regulated by
108 the septin-associated protein kinase Gin4 (31), thereby exerting cell cycle-dependent fine-tuning
109 of the leaflet lipid composition at the bud neck. However, other observations suggest that, aside
110 from stimulating flippases, Fpk1 (and Fpk2) act on other substrates. First, a triple mutant lacking
111 Fpk1, Fpk2, and Lem3, an accessory protein required for PM insertion and function of Dnf1 and
112 Dnf2 (29,30), has a much more severe growth defect than either a *lem3*Δ single mutant or an
113 *fpk1*Δ *fpk2*Δ double mutant (28). Second, Fpk1 phosphorylates Ypk1 at two N-terminal sites in a
114 sphingolipid-dependent manner; but, no marked effect on Ypk1 function appears to result from
115 these modifications (23). Third, independent of their action on either Ypk1 or the flippases, Fpk1
116 (and Fpk2) have been implicated in regulation of actin polarization and endocytosis (32);
117 however, no new substrate(s) was identified.

118 Here we document that Fpk1 phosphorylates and negatively regulates the protein kinase
119 Akl1. Akl1 (1,108 residues) is significantly larger than, but most closely related in its catalytic
120 domain to, the protein kinases Ark1 (638 residues) and Prk1 (810 residues). Ark1 and Prk1
121 appear to be necessary for uncoating of endocytic vesicles (33), and their orthologs (AAK1 and
122 GAK1) are involved in regulation of clathrin-mediated endocytosis in animal cells (34). We show
123 further that down-modulation of Akl1 by Fpk1 contributes to the efficiency of endocytosis. Our
124 findings define a new physiologically important substrate for Fpk1 and delineate another direct
125 mechanism by which TORC2-Ypk1 signaling (in this case, via its effect on Fpk1 activity)
126 regulates endocytosis, a process intimately coupled to maintenance of PM homeostasis.
127
128

MATERIALS AND METHODS

Strains and growth conditions. Yeast strains used in this study (Table 1) were grown routinely at 30˚C, unless otherwise indicated. Yeast were cultivated on standard rich (YP) medium or on a defined minimal (SC) medium (35) supplemented with appropriate nutrients to maintain selection for plasmids, using 2% glucose (Glc) as the carbon source, unless otherwise indicated. For gene induction from the *GAL1* promoter, cells were pre-grown to mid-exponential phase in SC containing 2% raffinose and 0.2% sucrose, galactose (Gal) was added (2% final concentration), and incubation was continued for 3 h. When cells were treated with myriocin (Myr) (Sigma-Aldrich Co., St. Louis, MO, USA) or phytosphingosine (PHS) (Avanti Polar Lipids, Inc., Alabaster, AL, USA), the cultures were grown to mid-exponential phase, induced with Gal for 1 h, the compounds added at the final concentrations indicated [Myr (1.25 μM) and PHS (10 μM)], and incubation was continued for an further 2 h. Standard yeast genetic methods were used for strain construction (35).

Plasmids and recombinant DNA methods. Plasmids used in this study (Table 2) were constructed using standard procedures (36) in *E. coli* strain DH5α. Fidelity of all constructs was verified by nucleotide sequence analysis. All PCR reactions were performed using Phusion™ DNA polymerase (ThermoFisher Scientific, Inc., Waltham, MA, USA) or high-fidelity KOD Hot Start™ DNA polymerase (EMD Millipore, Billerica, MA, USA). Site-directed mutagenesis using synthetic mismatch oligonucleotide primers, as appropriate, was conducted using the QuickChange™ method (Agilent Technologies, Inc., Santa Clara CA).

Preparation of cell extracts and immunoblotting. The cells in samples (1.5 ml) of an exponentially-growing culture ($A_{600\ nm}$ = 0.6) were collected by brief centrifugation, immediately frozen in liquid N_2 and then lysed by resuspension in 150 μl of 1.85 M NaOH, 7.4% β-mercaptoethanol. Protein in the resulting lysate was precipitated by the addition of 150 μl of 50% trichloroacetic acid on ice. After 10 min, the resulting denatured protein was collected by centrifugation, washed twice with acetone, solubilized by resuspension in 80 μl of 5% SDS in

0.1 M Tris base, and then 20 µl of a 5X stock of SDS-PAGE sample buffer was added. After boiling for 5 min, portions (15 µl) of the samples of interest were resolved electrophoretically, as follows: GFP-Akl1 or GFP-Akl1(Δ30-750) on a Phos-tag gel [8% acrylamide, 29:1 monomer-to-crosslinker, 23 µM Phos-tag™ reagent (Wako Pure Chemical Industries, Ltd., Osaka, Japan)]; Akl1-mCherry, Akl1-3XFLAG, or Ypk1-3XHA by SDS-PAGE (8% acrylamide, 29:1 monomer-to-crosslinker); 3XFLAG-Sla1(851-1244) by SDS-PAGE (10% acrylamide, 79:1 monomer-to-crosslinker); and, Ent2-GFP on a Phos-tag gel (8% acrylamide, 29:1 monomer-to-crosslinker, 10 µM Phos-tag™ reagent). For immunoblotting, the resolved proteins were transferred to nitrocellulose paper and the resulting filters incubated with appropriate primary antibodies in Odyssey™ buffer (Li-Cor Biosciences, Inc., Lincoln, NE, USA), washed, incubated with appropriate secondary antibodies conjugated to infrared fluorophores, and visualized using an Odyssey™ infrared imaging system (Li-Cor Biosciences). Antibodies used (dilution indicated) were: mouse anti-FLAG mAb M2 (1:10,000; Sigma-Aldrich); mouse anti-GFP mAb (1:1,000; Roche Diagnostics, Inc., Indianapolis, IN, USA); anti-RFP (1:10,000; Rockland Immunochemicals, Inc., Boyertown, PA, USA); rabbit polyclonal anti-Ypk1 phospho-T662 antibodies (9) [1:20,000; gift of Ted Powers, Univ. of California, Davis]; mouse monoclonal anti-HA.11 epitope antibody (1:10,000; BioLegend, Inc., San Diego, CA, USA); and, rabbit anti-Pgk1 [1:10,000; this lab, prepared as described in (37)].

Expression and purification of GST-Fpk1-6XHis. GST-Fpk1-6XHis, or a kinase-dead derivative, GST-Fpk1(D621A)-6XHis, was expressed from vector pGEX4T-1 (GE HealthCare Life Sciences, Chicago, IL, USA) in *E. coli* strain BL21(DE3). Bacterial cultures (1 L) in Luria-Bertani (LB) broth supplemented with ampicillin to select for the expression plasmid were grown to mid-exponential phase ($A_{600\,nm}$ = ~0.7) and protein production induced by addition of 1.2 mM isopropyl-β-d-thiogalactoside. After incubation with vigorous aeration for 6 h at 30˚C in a controlled temperature room, the cells were collected by centrifugation and washed with 30 mL

of ice-cold lysis buffer [phosphate-buffered saline (pH 7.4), 2 mM $MgCl_2$, 1 mM EDTA, 0.5% (v/v) Tween-20, 1x cOmplete protease inhibitors (Roche)] and recollected by centrifugation. The cell pellet was then frozen in liquid N_2 and stored at -80 ˚C. Cells were subsequently thawed in 50 mL of ice-cold lysis buffer and ruptured at 4˚C by sonication using an acoustic cell disrupter (model W185D, Branson Ultrasonics Corp., Danbury, CT, USA). The resulting lysate was clarified by centrifugation at 13,000xg for 30 min at 4˚C. The clarified extract was then incubated with 2 ml of a slurry of glutathione-agarose beads (GE HealthCare Life Sciences) in PBS (1:1) for 1.5 h at 4˚C. The mixture was then decanted into a glass column (1.5 cm diameter; Bio-Rad Laboratories, Inc., Hercules, CA, USA). After removal of the flow-through, the resin bed was rinsed with 10 ml of wash buffer [phosphate buffered saline (pH 7.4), 1 mM DTT, 0.1%(v/v) Tween-20] and the bound protein was eluted by addition of 3 mL of wash buffer containing 30 mM freshly dissolved glutathione. The protein eluate was diluted with 6 ml of HisA buffer [phosphate buffered saline (pH 7.4), 0.1% (v/v) Tween-20, 20 mM imidazole] and loaded using the 10-ml loop onto a 1-ml HisTRAP HP column in an AKTA™ FPLC system (GE Healthcare Life Sciences). The column was eluted with a linear gradient of HisA buffer to HisB buffer [phosphate buffered saline (pH 7.4), 0.1% (v/v) Tween-20, 500 mM imidazole] and fractions were collected. The proteins present in each fraction were resolved by SDS-PAGE and visualized by staining with Coomassie Blue dye. The peak fractions containing the highest concentrations of GST-Fpk1-6XHis [or GST-Fpk1(D621A)-6XHis] were pooled and, to exchange the buffer, the purified protein was passed over a PD-10 desalting column (GE Healthcare Life Sciences) pre-equilibrated in storage buffer [50 mM Tris-Cl (pH 7.5), 150 mM NaCl, 20% glycerol]. Aliquots of the purified protein solution were frozen in liquid N_2 and stored at -80 ˚C. Protein concentration was determined by the Bradford assay method (Bio-Rad) and the degree of purity assessed by SDS-PAGE followed by Coomassie staining.

Expression and purification of GST-Akl1(767-1108) and GST-Sla1(854-918). Freshly transformed *E. coli* BL21(DE3) cells carrying a plasmid expressing the desired GST-fusion

protein were grown to A_{600nm} = 0.6 and protein production was induced by addition of isopropyl-β-D-thiogalactopyranoside (0.6 mM final concentration). After vigorous aeration for 4 h at 30˚C, cells were harvested and the GST-fusion protein was purified by column chromatography on glutathione-agarose beads using the procedure described in the preceding section.

Protein kinase assay in solution. Purified GST-Fpk1-6XHis, or the kinase-dead derivative, GST-Fpk1(D621A)-6XHis, were incubated at 30˚C in protein kinase assay buffer [125 mM K-acetate, 12 mM $MgCl_2$, 0,5 mM EDTA, 0.5 mM EGTA, 2 mM DTT, 1% glycerol, 0.02% BSA, 25 mM β-glycerol phosphate, 1 mM sodium orthovanadate, 20 mM Tris-HCl (final pH 7.2)] with 100 μM [γ-^{32}P]ATP (~5 x 10^5 cpm/nmole) and 0.5 μg of purified GST-Akl1(767-1108). After 30 min, reactions were terminated by addition of SDS-PAGE sample buffer containing 6% SDS followed by boiling for 5 min. Labeled proteins were resolved by SDS-PAGE and analyzed by autoradiography using a PhosphorImager™ (Molecular Dynamics Div., Amersham Pharmacia Biotech, Inc., Piscataway, NJ, USA).

Immune-complex protein kinase assay. Cultures (40 ml) of yeast strain *akl1*Δ (YFR479) expressing either Akl1-3XFLAG (pFR316) or Akl1^{AA}-3XFLAG (pFR319) were grown to mid-exponential phase, collected by centrifugation, washed in ice-cold 1X PBS, resuspended in 0.2 ml of ice-cold IP buffer [20 mM Tris-HCl (pH 7.5), 125 mM K-acetate, 0.5 mM EDTA, 0.5 mM EGTA, 1 mM DTT, 0.1% Tween 20] containing protease inhibitors (Complete EDTA-free; Roche) and phosphatase inhibitors (25 mM β-glycerol phosphate and 1 mM sodium orthovanadate), lysed and immunoprecipitated with M2 anti-FLAG immunoglobulin-coated Protein A/G beads (Calbiochem-Novabiochem International, Inc., San Diego, CA, USA), as described previously (18). Bead-bound immune complexes were collected by centrifugation, washed once with IP buffer, twice with the kinase assay buffer described in the preceding section, resuspended in 20 μl of kinase assay buffer containing 100 μM [γ-^{32}P]ATP (~5 x 10^5 cpm/nmole) and incubated for 30 min with 0.5 μg of purified GST-Sla1(854-918). Reactions

were terminated by addition of SDS-PAGE sample buffer containing 6% SDS followed by boiling for 5 min. Labeled proteins were resolved and analyzed by autoradiography as described in the preceding section.

Subcellular localization by fluorescence microscopy. Yeast proteins fused to *Aequoria victoria* green fluorescent protein (GFP) (38) or *Discosoma sp.* red fluorescent protein (RFP) or its derivative mCherry (39) were constructed by in-frame integration at the corresponding chromosomal locus and expressed from the endogenous promoter. All such fusions were functional, as judged by the ability of the integrated construct to confer a normal phenotype. For routine visualization, yeast were grown to mid-exponential phase and viewed directly under an epifluorescence microscope (model BH-2; Olympus America, Inc., Center Valley, PA, USA) using a 100X objective equipped with appropriate band pass filters (Chroma Technology Corp., Rockingham, VT, USA). Images were collected using a charge-coupled device (CCD) camera (Photometrics, Inc., Tucson, AZ, USA), processed with μManager (40) and Photoshop™ (Adobe Systems, Inc., San Jose, CA, USA). In some experiments, to demarcate the PM, cells grown to mid-exponential phase were stained with CellMask Orange™ (5 μg/ml; ThermoFisher Scientific) for 2 min at room temperature and then images were taken with an Elyra PS.1 structured illumination fluorescence microscope (Carl Zeiss, Jena, Germany), equipped with a Zeiss 100x PlanApo 1.46NA TIRF objective, a main focus drive of the AxioObserver Z1 Stand, a WSB PiezoDrive 08 for super-resolution, and an Andor 512x512 EM-CCD camera (100nm x 100nm pixel size; Andor Technology, South Windsor, CT). GFP-tagged proteins were excited at 488 nm with an argon laser at 2.3% power (100 mW) and emission monitored in a 495-550 nm window. CellMask Orange™ was excited at 561 nm at 2.3% power (100 mW) and emission monitored in a 570-620 nm window. Images (average of 8 scans) were processed using ZEN software (Zeiss), ImageJ (NIH, Bethesda, MD, USA) (41), and Photoshop™ (Adobe).

Actin patch dynamics was monitored essentially as described (42) at 25°C in a temperature-controlled environmental chamber (In Vivo Scientific, St. Louis, MO). Lifetimes were analyzed

using ImageJ (NIH) and a plug-in that generates radial kymographs in 2-degree increments (http://www.embl.de/eamnet/html/body_kymograph.html).

RESULTS

Identifying and validating Fpk1 substrates. To date, the only known substrates of Fpk1 (and Fpk2) are: (i) the flippases Dnf1, Dnf2 and Dnf3 (hence, the name "Flippase Protein Kinase") (28); and, (ii) the protein kinase Ypk1 (23). We defined the consensus phospho-acceptor site for Fpk1 by determining what residues it phosphorylated in both Ypk1 and Dnf1. This motif is **R**-x-**S**-**Hpo**-**D/E**, where x represents any amino acid and Hpo represents a hydrophobic residue (L, I, V, M, F, Y, A) (23), and is in good accord with subsequent analysis of the phospho-acceptor site preference of Fpk1 (Ynr047w) using synthetic peptide arrays (43). Multiple copies (number indicated) of this motif are found in Dnf1 (six), Dnf2 (five), and Dnf3 (four), many of which have been detected as phosphorylated *in vivo* in genome-wide proteomic analyses (Table 3). We confirmed previously that two such sites (Ser1545 and Ser1552) in the C-terminal cytoplasmic tail of Dnf1 are robustly phosphorylated by Fpk1 *in vitro* (23). However, the physiological importance of phosphorylation at these sites had not been analyzed previously.

The flippases translocate aminoglycerophospholipids from the outer to the inner leaflet of the PM. The more phosphatidylethanolamine (PtdEth) in the outer leaflet, the more sensitive yeast cells are to the killing action of a PtdEth-binding antibiotic, duramycin (44). In the background of a cell in which Dnf2 and Dnf3 are absent, it is clear that Dnf1 makes a major contribution to the inward translocation of PtdEth because loss of Dnf1 makes yeast cells much more sensitive to killing by duramycin (Fig. 1A, *compare bottom panel to top panel*). Hence, as one approach to assess whether phosphorylation at its six Fpk1 sites affects Dnf1 function, we used the background of *dnf2*Δ *dnf3*Δ cells to compare the phenotypes of WT Dnf1 and Dnf1-GFP to corresponding site-directed mutants in which the Ser residues in all six Fpk1 motifs had been mutated to Ala. We found that, compared to WT Dnf1 or Dnf1-GFP, the Dnf1(6A) and Dnf1(6A)-GFP mutants were impaired for inward transport of PtdEth, as judged by the readily detectable increase in their sensitivity to duramycin (Fig. 1A). This difference was not attributable to any difference in either the level of expression of Dnf1(6A) compared to WT Dnf1

(Fig. 1B) or any difference in the localization pattern of Dnf1(6A)-GFP compared to Dnf1-GFP (Fig. 1C). We conclude that phosphorylation at its Fpk1 sites is indeed required for optimal Dnf1 function. [We have evidence that Dnf1 is also a MAPK substrate (Sartorel E, Roelants FM, Finnigan GC, Thorner J, manuscript in preparation); hence, we suspect that the prominent doublet observed, even for Dnf1(6A) lacking all of its Fpk1 sites (Fig. 1B), likely arises from its MAPK-dependent modification.]

Taking advantage of the observations and approaches described above, and cognizant of the indirect evidence that Fpk1 (and Fpk2) may have additional functions (28,32), we sought to identify previously uncharacterized Fpk1 substrates. To this end, we looked, first, for *S. cerevisiae* gene products that contain matches to the Fpk1 consensus phospho-acceptor motif using the Pattern Matching tool available at the *Saccharomyces* Genome Database (http://www.yeastgenome.org/cgi-bin/PATMATCH/nph-patmatch). Second, because Dnf1, Dnf2, Dnf3 and Ypk1 all contain multiple Fpk1 phosphorylation sites, we focused on candidates containing two or more predicted Fpk1 sites. Out of the more than 6,600 apparent ORFs encoded in the *S. cerevisiae* genome (http://www.yeastgenome.org/genomesnapshot), only 16 additional proteins contain at least two predicted Fpk1 phosphorylation sites (Table 3).

In particular, one potential candidate, the protein kinase Akl1, drew our attention for several reasons. First, the closest relatives of Akl1 are the protein kinases Ark1 and Prk1 (34), which are involved in regulation of endocytosis and actin cytoskeleton organization (33). Second, Rispal *et al.* (2015) (32) found evidence that Fpk1 (and Fpk2) are involved in these same processes, but the mechanism by which they contribute to endocytosis and actin organization was not determined. Third, endocytosis is clearly a process that is intimately connected to PM homeostasis, and we have recently demonstrated that cargo recognition molecules, α-arrestins, required for the endocytosis of integral PM proteins are, like Fpk1, under the direct control of TORC2-Ypk1 signaling (26).

Akl1 has an N-terminal catalytic domain (residues 25-320) and a long C-terminal extension

312 that contains near the C-terminus two canonical matches (**R**Q**S**^{960}**L**D and **R**Q**S**^{1072}**L**D) to the
313 consensus Fpk1 phospho-acceptor site motif, whereas Ark1 and Prk1 lack any such sequences
314 (Fig. 2A). Phosphorylation at both sites *in vivo* has been detected in genome-wide proteomic
315 analyses (Table 3). Moreover, the site corresponding to Ser960 in *S. cerevisiae* Akl1 is highly
316 conserved and the site corresponding to Ser1072 in *S. cerevisiae* Akl1 is completely conserved
317 in the other *sensu stricto Saccharomyces* species, as well as in more evolutionarily distant
318 yeasts (Fig. S1, *yellow boxes*). Furthermore, these sites have been conserved, despite the fact
319 the C-terminal extensions of the Akl1 orthologs of the more distantly related species have
320 clearly diverged substantially from that of *S. cerevisiae* Akl1, especially compared to the
321 relatively high degree of conservation of their respective kinase domains (Fig. S1). Interestingly,
322 two of the more distantly related yeasts (*S. castellii* and *Candida glabrata*) have each acquired a
323 third C-terminal consensus Fpk1 site (Fig. S1, *underlined in yellow*). Despite the very large
324 number of Arg residues in all of these proteins (>50), only those indicated at the immediate C-
325 terminal end, and nowhere else, correspond to an Fpk1 consensus phospho-acceptor site.
326 Hence, we sought to determine whether Akl1 is indeed a *bona fide* and physiologically relevant
327 substrate of Fpk1.
328 **Fpk1 phosphorylates Akl1**. We tested first whether Akl1 serves as a substrate for Fpk1 *in*
329 *vitro*. To avoid the possibility of self-phosphorylation, we generated and purified from *E. coli* a
330 GST-Akl1(767-1108) fusion corresponding to the C-terminal 341 residues of Akl1, which
331 contains its consensus Fpk1 sites (but lack its kinase domain). We found that GST-Akl1(767-
332 1108) incubated with purified recombinant Fpk1 and [γ-^{32}P]ATP was robustly phosphorylated,
333 but not when incubated with an equivalent amount of a catalytically-inactive Fpk1 mutant,
334 Fpk1(D621A), prepared in the same manner (Fig. 2B). The bulk of the phosphorylation occurred
335 at the Fpk1 consensus site corresponding to S960 because mutation of that residue to Ala
336 markedly reduced the amount of radioactivity incorporated, whereas mutation of S1072 to Ala
337 did not (Fig. 2B). However, the corresponding double mutant (S960A S1072A) exhibited a

338 further decrease in incorporation (Fig. 2B), indicating that both sites are phosphorylated *in vitro*.

339 To assess whether Akl1 is phosphorylated in an Fpk1-dependent manner *in vivo,* we initially
340 analyzed the migration pattern of full-length Akl1 (tagged at its N-terminus with GFP) on
341 phosphate affinity (Phos-tag) gels, in which phosphorylated isoforms are retarded in their
342 mobility with respect to the unmodified species (45). Indeed, in cell extracts, we reproducibly
343 detected slower mobility species, which were largely abrogated in either an Akl1(S960A
344 S1072A) double mutant or an *fpk1*Δ *fpk2*Δ double mutant (Fig. 2C). Slower mobility species also
345 were observed for full-length Akl1 tagged at its C-terminus with mCherry and eliminated by
346 treatment with phosphatase, confirming that they arose from phosphorylation (Fig. 2D). For
347 better resolution of such phospho-isoforms, we next examined the migration of a much smaller,
348 387-residue derivative, Akl1(Δ30-751). In agreement with the results for full-length Akl1, the
349 slowest mobility species were eliminated in an *fpk1*Δ *fpk2*Δ double mutant (Fig. 2E, *right*), as
350 well as by an Akl1(S960A S1072A) double mutation (Fig. 2E, *middle*). These species result from
351 phosphorylation because they were also eliminated by phosphatase treatment (Fig. 2F).
352 Interestingly, although the GFP-Akl1(Δ30-751) construct examined *in vivo* is largely congruent
353 with and not much larger than the 342-residue GST-Akl1(767-1108) C-terminal fragment used *in*
354 *vitro*, analysis of the effect of single mutations on the migration pattern indicated that, in the cell,
355 S1072 was the primary site for Fpk1-mediated phosphorylation (Fig. 2E, *left*), whereas S960
356 was the preferred site *in vitro* (Fig. 2B).

357 We demonstrated previously that Fpk1 is inhibited by the TORC2-activated protein kinase
358 Ypk1 (23). Therefore, we examined Akl1 phosphorylation in a strain background, *avo3*Δ*CT*
359 *TOR1-1* (46), in which only TORC2 can be inhibited by treatment of the cells with rapamycin,
360 whereupon Ypk1-mediated inhibition of Fpk1 should be abrogated. Indeed, in accord with our
361 expectations, we found that phosphorylation of Akl1 was increased upon addition of rapamycin
362 in these cells (Fig. 2G). Furthermore, analysis of the S960A, S1072A and S960A S1072A
363 mutants confirmed that this increase in phosphorylation occurs largely at the S1072 Fpk1 site

(Fig. 2H). These findings verify that Fpk1 is activated upon TORC2-Ypk1 inhibition and responsible for the observed increase in phosphorylation.

We have provided evidence previously that production of the complex sphingolipid mannosyl-inositolphosphorylceramide (MIPC) is required for maintenance of active Fpk1 *in vivo* (23). Correspondingly, we found that treatment of cells with myriocin (Myr), an antibiotic that inhibits sphingolipid biosynthesis (47), eliminated the slowest mobility Akl1 phospho-isoforms to an extent similar to that observed in cells lacking Fpk1 and Fpk2, whereas stimulating sphingolipid synthesis by exogenous addition of an excess of the long-chain base phytosphingosine (PHS) modestly elevated the slowest mobility Akl1 phospho-isoforms and required the presence of Fpk1 and Fpk2 to do so (Fig. 3A). Because blocking sphingolipid production also leads to activation of TORC2, which, in turn, stimulates Ypk1 (6,7), and Fpk1 is inhibited by Ypk1-mediated phosphorylation (23), it was possible that the apparent decrease in Fpk1 activity observed upon Myr treatment was due solely to upregulation of TORC2-Ypk1-mediated Fpk1 inhibition. However, Myr treatment still caused a marked decrease in the slowest mobility Akl1 phospho-isoforms in a strain expressing constitutively-active Ypk1(D242A) (6) and lacking Slm1 and Slm2 (Fig.3B) [which prevents TORC2-mediated phosphorylation of Ypk1 or Ypk2 (7,9)], as we confirmed (Fig. 3C and 3D)]. Conversely, Myr treatment still caused a marked decrease in the slowest mobility Akl1 phospho-isoforms in cells lacking Ypk1 altogether (Fig. 3B). Thus, production of the complex sphingolipid MIPC is needed for optimal Fpk1 activity, independent of the effect that sphingolipids also have on regulation of Fpk1 through TORC2-Ypk1.

Taken together, these collective observations demonstrate unequivocally that Fpk1 phosphorylates Akl1 *in vivo* in a manner responsive to the sphingolipid status of the PM.

Fpk1-mediated phosphorylation down-regulates Akl1 activity. We next sought to determine the effect that Fpk1-mediated phosphorylation has on Akl1 function. Downstream

substrates of Akl1 have been identified and are gene products involved in actin-patch mediated endocytosis (48): Sla1 (49), a protein required for assembly of cortical actin at endocytic sites (33,50); Pan1 (51,52), one component of a three-protein complex that stimulates actin filament assembly (53); and, Ent1 and Ent2 (54,55), PtdIns4,5P_2-, ubiquitinylated cargo-, and clathrin-binding proteins (56-58).

Sla1 contains 21 consensus Akl1/Prk1 phospho-acceptor site motifs (43,59), which are all confined to the C-terminal third of this protein (Fig. 4A). We confirmed that a purified recombinant fragment, GST-Sla1(854-918), containing five of these consensus Akl1/Prk1 sites was robustly phosphorylated by WT Akl1-3XFLAG immunoprecipitated from yeast cell extracts, but not by a catalytically-inactive mutant, Akl1(D181Y)-3XFLAG, prepared in the same manner (Fig. 4B). Hence as an initial approach to assess the influence of Fpk1-mediated phosphorylation on Akl1 activity, we examined the ability of either WT Akl1-3XFLAG or an equivalent amount of an Akl1(S960A S1072A)-3XFLAG mutant (in which both the Fpk1 phosphorylation sites were mutated to Ala) to phosphorylate GST-Sla1(854-918). A time course for these reactions revealed that Akl1(S960A S1072A)-3XFLAG both auto-phosphorylated and phosphorylated GST-Sla1(854-918) at a significantly faster rate and to a greater extent than WT Akl1-3XFLAG (Fig. 4C), and immunoblotting confirmed that the mutant and WT kinases were present in the same amount (Fig. 4D). Thus, at least as judged by such *in vitro* reactions, phosphorylation by Fpk1 is inhibitory to Akl1 function.

To confirm this conclusion *in vivo*, and allow for sensitive detection of phospho-isoforms, we examined the mobility of a 394-residue C-terminal fragment of Sla1, 3xFLAG-Sla1(851-1244), which contains 19 of its 21 Akl1 phosphorylation sites (Fig. 4A). We found that, in cells lacking Fpk1 and Fpk2, there was an increase in phosphorylation of this fragment, as judged by a readily detectable increase in slower mobility isoforms and by the marked diminution in the hypo-phosphorylated isoform, compared to the otherwise isogenic *FPK1*$^+$ *FPK2*$^+$ cells (Fig. 4E, *left*). The slower mobility species were all attributable to phosphorylation because these bands

were collapsed by phosphatase treatment (Fig, 4E, *left*). Likewise, in cells expressing Akl1 in which both of its Fpk1 consensus sites had been mutated to Ala, there was a similar increase in the slower mobility isoforms, compared to otherwise isogenic cells expressing WT Akl1 (Fig. 4E, *right*). To determine whether this effect was general and applied to other Akl1 substrates, we examined Ent2. Indeed, we saw the same trend; in cells lacking Fpk1 and Fpk2, there was an increase in Ent2 phosphorylation, as judged by an increase in slower mobility isoforms (Fig. 4F). These data indicate that when Fpk1-mediated phosphorylation is absent, Akl1 is more effective in phosphorylating its substrates in the cell, corroborating the conclusion of our *in vitro* analysis.

To make certain that these observed effects were mediated by the inhibition that Fpk1-dependent phosphorylation exerts on Akl1 activity *per se*, we examined the impact of Fpk1 function on the level and localization of Akl1. As judged by immunoblotting (and normalized to the loading control, Pgk1), the steady-state level of Akl1 was unaffected, regardless of whether cells expressed a hyper-active Fpk1 allele ($Fpk1^{11A}$), WT Fpk1, or lacked both Fpk1 and Fpk2 (Fig. 5A). $Fpk1^{11A}$ is hyper-active because it is not subject to negative regulation by Gin4 protein kinase (31). Likewise, when analyzed in the same manner, the levels of an allele lacking its Fpk1 sites, Akl1(S960A S1072A), or an allele mimicking phosphorylation at its Fpk1 sites, Akl1(S960E S1072E), were indistinguishable from WT Akl1 (Fig. 5B). Similarly, as judged by fluorescence microscopy, the subcellular distribution of Akl1-mCherry in a number of PM-associated puncta was equivalent in cells expressing WT Fpk1, or lacking Fpk1 and Fpk2, or expressing the hyperactive $Fpk1^{11A}$ allele (Fig. 5C). We conclude, therefore that Fpk1-mediated phosphorylation inhibits Akl1 function, but does not affect either its stability or its localization.

In the absence of negative regulation by Fpk1, Akl1 impedes endocytosis. As we have demonstrated here, Sla1 is a substrate for Akl1 both *in vitro* and *in vivo*. Sla1 is essential for proper formation of cortical actin patches (60) and is required for endocytosis (61). Proper execution of endocytosis clearly requires tight spatial and temporal control of a very large number of protein-membrane and protein-protein interactions (48). As for Akl1, all of the known

441 targets of its most closely related protein kinases, Ark1 and Prk1, are involved in clathrin- and
442 actin patch-mediated endocytosis, including Sla1, Pan1, Ent1, Ent2, Yap1801, Yap1802, and
443 Scd5 (49,54,59,62,63). We confirmed that Akl1-mediated phosphorylation down-regulates
444 endocytosis by looking, first, at fluid phase uptake of Lucifer Yellow CH (LY) into the vacuole
445 because prior studies established that this dye enters yeast via actin patch-dependent
446 endocytosis (64-66). We found that *akl1*Δ cells carrying an empty *GAL* promoter vector exhibit
447 very prominent LY staining of the vacuole on galactose medium, whereas the same cells
448 expressing Akl1(S960A S1072A) from the *GAL* promoter showed a marked reduction in LY
449 staining of the vacuole, but expression at an equivalent level of a catalytically-inactive
450 derivative, Akl1(D181A S960A S1072A) did not (Fig. 6A). Moreover, Akl1 localized in cortical
451 "dots" (Fig. 6A), presumably reflecting association with endocytic actin patches, as observed for
452 Ark1 and Prk1 (67). Co-localization of Akl1-mCherry with Sla1-GFP confirmed this conclusion
453 (Fig. 6B). The actions of Ark1 and Prk1 are thought to be involved in recycling of endocytic
454 factors because, in the absence of Ark1 and Prk1, cortical patches containing actin, clathrin and
455 other endocytic components aggregate at the cell cortex (68) and also accumulate as large
456 clumps in the cytosol (67,69).

457 For these reasons, as a test of whether Fpk1 phosphorylation of Akl1 has any effect on
458 endocytosis, we monitored the lifetime of Sla1-GFP at cortical actin patches in cells expressing
459 wild-type Akl1 or the hyperactive Akl1(S960A A1072A) allele that is immune to Fpk1-mediated
460 inhibition (Fig. 6C; see also Supplemental Movies 1 and 2). Strikingly, even though these same
461 cells contained WT Ark1 and Prk1, there was a modest (11%), yet reproducible and statistically
462 significant (students t-test, $p = 0.001$), reduction in the time that Sla1-GFP remained at cortical
463 actin patches in cells expressing Akl1(S960A A1072A), compared to cells expressing WT Akl1
464 (Fig 6D), even though the percentage of patches internalized did not vary between cells
465 expressing WT Akl1 and those expressing Akl1(AA) (Fig. 6E). Thus, when not subject to Fpk1-
466 mediated inhibition, Akl1 causes faster dissociation of Sla1 from endocytic sites.

Aside from sequence homology of its kinase domain to that in Ark1 and Prk1, Akl1 was also identified as a gene that, when overexpressed, rendered *S. cerevisiae* resistant to the toxic effects of doxorubicin (51). The following evidence supports the conclusion that this phenotype arises, in large measure, via inhibition of endocytosis. Overexpression of Prk1 also conferred elevated resistance to doxorubicin (51), and it has been shown that elevated Prk1 inhibits endocytosis by dissociating the Sla1/Pan1/End3 complex via phosphorylation of both Sla1 and Pan1 (49,52). As we have corroborated here, Sla1 is also an efficient substrate for Akl1 and others have shown that Pan1 is a substrate of Akl1 (51). Consistent with this conclusion, Sla1- and End3-defective mutants also exhibited elevated resistance to doxorubicin (51). Conversely, and also consistent with a role for Akl1 in preventing doxorubicin entry by blocking endocytosis, *akl1*Δ cells are hypersensitive to this antibiotic (51,70,71).

Given the role we uncovered for Fpk1 in phosphorylating and negatively regulating Akl1, as a second independent test of whether phosphorylation of Akl1 by Fpk1 has an impact on endocytosis, we examined the effects of doxorubicin on cells with different levels of Fpk1 activity. We found first that cells expressing the hyperactive Fpk1^{11A} allele, which should reduce Akl1 activity and enhance endocytosis, are more sensitive to this compound than otherwise isogenic WT cells (but, not as sensitive as an *akl1*Δ null mutant) and, conversely, cells lacking Fpk1 and Fpk2, which should permit elevated Akl1 activity and inhibit endocytosis, are more resistant to the compound than WT cells (Fig. 7A, *upper panel*). Thus, by this criterion too, Fpk1 modulation of Akl1 activity does influence the efficiency of endocytosis. On the other hand, because Fpk1 also phosphorylates and stimulates the flippases Dnf1 and Dnf2 (28) and because flippase function affects cell permeability to other xenobiotics agents (31,72), we tested the effects of doxorubicin on cells lacking the flippases. We found that *dnf1*Δ *dnf2*Δ *dnf3*Δ were more doxorubicin resistant that otherwise isogenic WT cells and displayed a degree of resistance quite comparable to that of *fpk1*Δ *fpk2*Δ cells (Fig. 7A, *lower panel*). Hence, the effects of changes in Fpk1 activity may yield the observed doxorubicin phenotypes through its

493 regulation of Akl1 or its regulation of the flippases, or both.

494 To try to deconvolute these two aspects of Fpk1 function, we compared the doxorubicin
495 sensitivity of *FPK1*$^{+}$ *FPK2*$^{+}$ cells, which should have normal regulation of flippase function,
496 expressing WT Akl1, or an Akl1 allele that cannot be phosphorylated by Fpk1, which we have
497 shown to be hyperactive compared to WT Akl1, or an Akl1 allele that mimics permanent
498 phosphorylation by Fpk1, which we presumed would be crippled for function compared to WT
499 Akl1. We found that cells expressing the hyperactive Akl1(S960A S1072A) allele were
500 reproducibly somewhat more resistant to doxorubicin than cells expressing WT Akl1 (Fig. 7B).
501 Thus, in the absence of negative regulation of Akl1 by Fpk1, the increase in phosphorylation of
502 endocytic proteins by Akl1 impedes endocytosis, enhancing doxorubicin resistance. This
503 scenario predicts that an Akl1 mutant that mimics permanent phosphorylation by Fpk1 might be
504 more sensitive to this antibiotic than wild-type cells. However, cells expressing Akl1(S960E
505 S1072E) were just as resistant to doxorubicin as cells expressing Akl1(S960A S1072A). We
506 presume that Glu (or Asp) substitutions are, in this case, not a good mimic for authentic
507 phosphorylation, as others (73) and we ourselves (21,22) have encountered, on occasion, for
508 certain other phospho-proteins.

509 Cells lacking Akl1 also exhibit greater sensitivity to the killing action of hygromycin B (74).
510 Consistent with our other findings indicating that Akl1(S960A S1072A), which cannot be
511 phosphorylated by Akl1, is hyperactive, we found that Akl1(S960A S1072A) conferred greater
512 resistant to hygromycin B than WT Akl1 (Fig. 7D). Furthermore, prolonged overexpression of
513 Akl1 is toxic to cells (75) and, in further accord with the conclusion that Akl1(S960A S1072A) is
514 hyperactive, its overexpression was even more toxic than overexpression of WT Akl1 (Fig. 7D,
515 *left side*). However, a decrease in sphingolipid levels causes a drastic reduction of Fpk1 activity
516 (23) due to the decrease in the Fpk1 activator MIPC (Fig. 3), as well as to the increase in
517 TORC2-stimulated Ypk1 activity (6) and the ensuing Ypk1-mediated inhibitory phosphorylation
518 of Fpk1 (23). Under these conditions, its Fpk1-mediated negative regulation should be alleviated

519 and, thus, Akl1 maximally active. Consistent with this model, we found that, in the presence of
520 the sphingolipid biosynthesis inhibitor myriocin, overexpression of WT Akl1 was just as toxic as
521 overexpression of Akl1(S960A S1072A) (Fig. 7D, *right side*).
522
523
524

DISCUSSION

Our findings document that Fpk1 phosphorylates two consensus sites at the C-terminal end of Akl1 *in vitro* and *in vivo*, and further that this Fpk1-mediated phosphorylation of Akl1 exerts negative regulation that has a readily detectable and physiologically important effect on Akl1 function. When relieved of Fpk1-mediated inhibition, Akl1 action inhibits endocytosis, as judged by more rapid dissociation of an endocytic factor from endocytic sites, elevated doxorubicin resistance, and a reduced rate of LY uptake. Therefore, stimuli that reduce Fpk1 activity, such as sphingolipid depletion and other PM stresses that activate TORC2-Ypk1 action, or cell cycle-dependent activation of protein kinase Gin4, which also phosphorylates and negatively regulates Fpk1 (31), will down-modulate the efficiency of endocytosis (Fig. 8). This response perhaps makes biological sense, in that cells would avoid drastic removal of PM constituents while undergoing other processes to cope with the stress.

Until now, Akl1 was the least studied of the three Ark1 and Prk1 family protein kinases, mainly because lack of both Ark1 and Prk1 causes a prominent endocytic defect and major actin assembly aberrations, which are not observed when Akl1 is deleted, either alone or in combination with either an *ark1*Δ or *prk1*Δ mutation (67,69). Thus, under otherwise normal growth conditions, Akl1 makes, at most, only a minor contribution to modulating actin patch-mediated endocytosis. However, our results reveal that the role of Akl1 is to provide a mechanism whereby cells can down-modulate the efficiency of endocytosis in response to membrane stress. The factor that couples Akl1 to these stress response pathways is the protein kinase Fpk1, whose activity is, in turn, a nodal point for inputs from several upstream signaling pathways (Fig. 8).

A recent study (32) also linked TORC2 activity to the phosphorylation state of Akl1; but, that study reported, contrary to our findings, that Akl1 was *less* phosphorylated when TORC2 was inhibited. In their global mass spectrometry analysis, however, the only residue hypophosphorylated upon TORC2 inhibition was -EQ**S**^{504}PR-, which is likely a Cdk1 site

because it has been shown to be modified in a *CDC28*-dependent manner *in vivo* (76), and is not well conserved among Akl1 orthologs (Fig. S1). Apparently, Rispal et al. (2015) did not detect phosphorylation sites in Akl1 that increased.

Given the regulatory circuit we have described here (Fig. 8), inhibition of TORC2 should reduce phosphorylation of authentic Akl1 substrates. However, any such changes are likely masked by the fact that Ark1 and especially Prk1 share the same consensus phospho-acceptor motif and are not under the same regulation. In agreement with this view, in the mass spectrometry analysis of Rispal et al. (2015), Sla1, a protein that we demonstrated here is a *bona fide* Akl1 substrate both *in vitro* and *in vivo*, did not show any diminution of phosphorylation at its Akl1/Prk1 consensus sites after TORC2 inhibition. Interestingly, they did observe hypophosphorylation within peptide sequences in Sla1 that contain its consensus Ypk1 phospho-acceptor site motifs (Fig. 4A), suggesting that Sla1 might also be a direct target of Ypk1. However, Rispal *et al.* (2015) were unable to show direct phosphorylation of Sla1 by Ypk1 *in vitro* (32) and over-expression of Sla1 is not growth-inhibitory when Ypk1 activity is limiting, a hallmark of many demonstrated Ypk1 substrates (8). Nonetheless, in a recent global proteomics study (77), myriocin treatment, which activates TORC2 and Ypk1 (6), increased Sla1 phosphorylation at S449, a candidate Ypk1 site (Fig. 4A).

Most strikingly, we have shown here that the C-terminal 394 residues of Sla1, which contain 19 of its 21 Akl1/Prk1 consensus sites (but no Ypk1 consensus site; Fig. 4A) is clearly hyperphosphorylated when Akl1 cannot be phosphorylated by Fpk1 (Fig. 4E). Thus, as we have shown for Sla1 (Fig. 6C and D), stress-induced activation of the TORC2→Ypk1—|Fpk1—|Akl1 kinase circuit will increase phosphorylation of other endocytic factors by Akl1, causing their premature dissociation, thereby impeding clathrin- and actin patch-mediated endocytosis. In agreement with this conclusion, it has been shown recently (78) that a Sla1 derivative lacking 10 of its 21 C-terminal Akl1/Prk1 phosphorylation sites has a substantially longer dwell time on

cortical actin patches than WT Sla1.

Several other candidate Fpk1 substrates (Table 3) have described roles in processes that could affect the efficiency of endocytosis indirectly because adequate sphingolipid and sterol production are both required for normal endocytic events (79,80). For example, Vps54 is a component of the GARP complex, which has recently been shown to be required for sphingolipid homeostasis (81); Lcb5 is a long-chain (sphingoid) base kinase (82); and, Erg1 is the squalene mono-oxygenase that generates the squalene epoxide required for ergosterol biosynthesis (83). Further study of such putative Fpk1 substrates could deepen our understanding of how the TORC2-Ypk1-Fpk1 signaling circuit controls PM homeostasis.

We found that hyperactive Akl1 enhances resistance to doxorubicin, a widely used cytotoxic anti-cancer medicine. As with many chemotherapic agents, acquisition of resistance is a major problem. Doxorubicin resistance in human cells is due, in some cases, to up-regulation of ABC transporters (multi-drug resistance pumps) MRP1 (84) and MDR1/P-glycoprotein (85), but other proteins also have been implicated (86,87). A prior study in *S. cerevisiae* was the first to show that over-expression of either Akl1 or Prk1, and consequent inhibition of endocytosis, conferred enhanced resistance to doxorubicin (51). The same study reported that over-expression of AAK1, a human Ark1/Prk1-related family member, conferred elevated doxorubicin resistance in human cells (51). Thus, in a therapeutic setting, use of kinase inhibitors that inhibit AAK1 and GAK1 activity might enhance the effectiveness of doxorubicin as an anti-tumor agent. In this same regard, as we have shown here (Fig. 3), maintenance of high Fpk1 activity (and, thus, inhibition of Akl1) requires robust sphingolipid biogenesis and, in accordance, cells lacking Orm2, which increases metabolic flux into sphingolipid biosynthesis (27,88), are more sensitive to doxorubicin than wild-type cells (89).

We also showed here that deletion of Dnf1, Dnf2 and Dnf3 renders cells highly resistant to doxorubicin (Fig. 7A), highlighting the importance of flippase action and thus the outer and inner leaflet aminoglycerophospholipid composition in sensitivity to this drug. It was suggested that

602 flippases have a direct role in endocytosis (90), but it seems more likely that flippase action
603 modulates the leaflet lipid composition thereby influencing the efficiency with which xenobiotic
604 agents partition into and cross the PM permeability barrier. The bilayer lipid distribution likely
605 also influences membrane protein composition, distribution and/or orientation, with consequent
606 effects on the content and function of many integral PM-localized proteins, like drug efflux
607 pumps. Pdr5, the ABC transporter most responsible for pleiotropic drug resistance in *S.*
608 *cerevisiae*, has been implicated in doxorubicin resistance (71,91-93), but direct interactions
609 between flippases and Pdr5 (or other PM-localized ABC transporters) have been reported (94-
610 96). Therefore, the resistance to doxorubicin of cells over-expressing Pdr5 (97) may not be due
611 solely to increased Pdr5-mediated ejection of the drug, but possibly to negative effects on
612 flippase activity caused by elevated Pdr5.
613
614
615
616
617
618
619

ACKNOWLEDGMENTS

This work was supported by NIH R01 Research Grant GM21841 (to J.T.). We thank Ken Wolfe (University College, Dublin, Ireland), Chris Hittinger (Univ. of Wisconsin, Madison, WI, USA), Mark Johnston (Univ. of Colorado Sch. of Med., Aurora, CO, USA) and Jasper Rine (Univ. of California, Berkeley, CA, USA) for valuable advice about yeast genomics, Todd Graham (Vanderbilt Univ, Nashville, TN, USA) and Robbie Loewith (Univ. of Geneva, Switzerland) for the gift of strains, Ted Powers (Univ. of California, Davis, CA, USA) for the gift of plasmids and anti-Ypk1 phospho-T662 antibodies, Dr. Steven Ruzin (Biological Imaging Facility, College of Natural Resources, Univ. of California, Berkeley, CA, USA) and Anita Emmerstorfer-Augustin (this laboratory) for assistance with structured illumination microscopy, and especially David Drubin (Univ. of California, Berkeley, CA, USA) for strains, plasmids and the generous contribution of the expertise of his laboratory in analyzing the dynamics of actin patch-mediated endocytosis in yeast.

REFERENCES

1. Brennwald, P., and Rossi, G. (2007) Spatial regulation of exocytosis and cell polarity: yeast as a model for animal cells. *FEBS Lett.* **581**, 2119-2124.
2. Platta, H. W., and Stenmark, H. (2011) Endocytosis and signaling. *Curr. Opin. Cell Biol.* **23**, 393-403.
3. Groves, J. T., and Kuriyan, J. (2010) Molecular mechanisms in signal transduction at the membrane. *Nat. Struct. Mol. Biol.* **17**, 659-665.
4. Henry, S. A., Gaspar, M. L., and Jesch, S. A. (2014) The response to inositol: regulation of glycerolipid metabolism and stress response signaling in yeast. *Chem. Phys. Lipids* **180**, 23-43.
5. Olson, D. K., Fröhlich, F., Farese, R. V. J., and]Walther, T. C. (2016) Taming the sphinx: Mechanisms of cellular sphingolipid homeostasis. *Biochim. Biophys. Acta* **1861**, 784-792.
6. Roelants, F. M., Breslow, D. K., Muir, A., Weissman, J. S., and Thorner, J. (2011) Protein kinase Ypk1 phosphorylates regulatory proteins Orm1 and Orm2 to control sphingolipid homeostasis in Saccharomyces cerevisiae. *Proc. Natl. Acad. Sci. USA* **108**, 19222-19227.
7. Berchtold, D., Piccolis, M., Chiaruttini, N., Riezman, I., Riezman, H., Roux, A., Walther, T. C., and Loewith, R. (2012) Plasma membrane stress induces relocalization of Slm proteins and activation of TORC2 to promote sphingolipid synthesis. *Nat. Cell Biol.* **14**, 542-547.
8. Muir, A., Ramachandran, S., Roelants, F. M., Timmons, G., and Thorner, J. (2014) TORC2-dependent protein kinase Ypk1 phosphorylates ceramide synthase to stimulate synthesis of complex sphingolipids. *Elife* **3**, e03779.1-e03779.34.
9. Niles, B., Mogri, H., Hill, A., Vlahakis, A., and Powers, T. (2012) Plasma membrane recruitment and activation of the AGC kinase Ypk1 is mediated by target of rapamycin complex 2 (TORC2) and its effector proteins Slm1 and Slm2. *Proc. Natl. Acad. Sci. USA* **109**, 1536-1541.
10. Sun, Y., Miao, Y., Yamane, Y., Zhang, C., Shokat, K. M., Takematsu, H., Kozutsumi, Y., and Drubin, D. G. (2012) Orm protein phosphoregulation mediates transient sphingolipid biosynthesis response to heat stress via the Pkh-Ypk and Cdc55-PP2A pathways. *Mol. Biol. Cell* **23**, 2388-2398.

11. Lee, Y. J., Jeschke, G. R., Roelants, F. M., Thorner, J., and Turk, B. E. (2012) Reciprocal phosphorylation of yeast glycerol-3-phosphate dehydrogenases in adaptation to distinct types of stress. *Mol. Cell. Biol.* **32**, 4705-4717.
12. Muir, A., Roelants, F. M., Timmons, G., Leskoske, K. L., and Thorner, J. (2015) Down-regulation of TORC2-Ypk1 signaling promotes MAPK-independent survival under hyperosmotic stress. *Elife* **4**, 09336.1-09336.13.
13. Fadri, M., Daquinag, A., Wang, S., Xue, T., and Kunz, J. (2005) The pleckstrin homology domain proteins Slm1 and Slm2 are required for actin cytoskeleton organization in yeast and bind phosphatidylinositol-4,5-bisphosphate and TORC2. *Mol. Biol. Cell* **16**, 1883-1900.
14. Bultynck, G., Heath, V. L., Majeed, A. P., Galan, J. M., Haguenauer-Tsapis, R., and Cyert, M. S. (2006) Slm1 and slm2 are novel substrates of the calcineurin phosphatase required for heat stress-induced endocytosis of the yeast uracil permease. *Mol. Cell. Biol.* **26**, 4729-4745.
15. Tabuchi, M., Audhya, A., Parsons, A. B., Boone, C., and Emr, S. D. (2006) The phosphatidylinositol 4,5-biphosphate and TORC2 binding proteins Slm1 and Slm2 function in sphingolipid regulation. *Mol. Cell. Biol.* **26**, 5861-5875.
16. Douglas, L. M., and Konopka, J. B. (2014) Fungal membrane organization: the eisosome concept. *Annu. Rev. Microbiol.* **68**, 377-393.
17. Chen, P., Lee, K. S., and Levin, D. E. (1993) A pair of putative protein kinase genes (*YPK1* and *YPK2*) is required for cell growth in *Saccharomyces cerevisiae*. *Mol. Gen. Genet.* **236**, 443-447.
18. Roelants, F. M., Torrance, P. D., Bezman, N., and Thorner, J. (2002) Pkh1 and Pkh2 differentially phosphorylate and activate Ypk1 and Ykr2 and define protein kinase modules required for maintenance of cell wall integrity. *Mol. Biol. Cell* **13**, 3005-3028.
19. Kamada, Y., Fujioka, Y., Suzuki, N. N., Inagaki, F., Wullschleger, S., Loewith, R., Hall, M. N., and Ohsumi, Y. (2005) Tor2 directly phosphorylates the AGC kinase Ypk2 to regulate actin polarization. *Mol. Cell. Biol.* **25**, 7239-7248.
20. Aronova, S., Wedaman, K., P.A., A., Fontes, K., Ramos, K., Hammock, B. D., and Powers, T. (2008) Regulation of ceramide biosynthesis by TOR complex 2. *Cell Metab.* **7**, 148-158.
21. Casamayor, A., Torrance, P. D., Kobayashi, T., Thorner, J., and Alessi, D. R. (1999) Functional counterparts of mammalian protein kinases PDK1 and SGK in budding yeast. *Curr. Biol.* **9**, 186-197.

22. Roelants, F. M., Torrance, P. D., and Thorner, J. (2004) Differential roles of PDK1- and PDK2-phosphorylation sites in the yeast AGC kinases Ypk1, Pkc1 and Sch9. *Microbiology* **150**, 3289-3304.
23. Roelants, F. M., Baltz, A. G., Trott, A. E., Fereres, S., and Thorner, J. (2010) A protein kinase network regulates the function of aminophospholipid flippases. *Proc. Natl. Acad. Sci. USA* **107**, 34-39
24. Kunz, J., Henriquez, R., Schneider, U., Deuter-Reinhard, M., Movva, N. R., Hall, M. N., and 7;73(3):, C. M. (1993) Target of rapamycin in yeast, TOR2, is an essential phosphatidylinositol kinase homolog required for G1 progression. *Cell* **73**, 585-596.
25. Helliwell, S. B., Wagner, P., Kunz, J., M., D.-R., Henriquez, R., and Hall, M. N. (1994) TOR1 and TOR2 are structurally and functionally similar but not identical phosphatidylinositol kinase homologues in yeast. *Mol. Biol. Cell* **5** 105-118.
26. Alvaro, C. G., Aindow, A., and Thorner, J. (2016) Differential phosphorylation provides a switch to control how α-arrestin Rod1 down-regulates mating pheromone response in *Saccharomyces cerevisiae*. *Genetics* **203**, 299-317.
27. Breslow, D. K., Collins, S. R., Bodenmiller, B., Aebersold, R., Simons, K., Shevchenko, A., Ejsing, C. S., and Weissman, J. S. (2010) Orm family proteins mediate sphingolipid homeostasis. *Nature* **463**, 1048-1053.
28. Nakano, K., Yamamoto, T., Kishimoto, T., Noji, T., and Tanaka, K. (2008) Protein kinases Fpk1p and Fpk2p are novel regulators of phospholipid asymmetry. *Mol. Biol. Cell* **19**, 1783-1797.
29. Sebastian, T. T., Baldridge, R. D., Xu, P., and Graham, T. R. (2012) Phospholipid flippases: building asymmetric membranes and transport vesicles. *Biochim. Biophys. Acta* **1821**, 1068-1077.
30. Andersen, J. P., Vestergaard, A. L., Mikkelsen, S. A., Mogensen, L. S., Chalat, M., and Molday, R. S. (2016) P4-ATPases as phospholipid flippases-structure, function, and enigmas. *Front. Physiol.* **7**, 275.1—275.23.
31. Roelants, F. M., Su, B. M., von Wulffen, J., Ramachandran, S., Sartorel, E., Trott, A. E., and Thorner, J. (2015) Protein kinase Gin4 negatively regulates flippase function and controls plasma membrane asymmetry. *J. Cell Biol.* **208**, 299-311.
32. Rispal, D., Eltschinger, S., Stahl, M., Vaga, S., Bodenmiller, B., Abraham, Y., Filipuzzi, I., Movva, N. R., Aebersold, R., Helliwell, S. B., and Loewith, R. (2015) Target of Rapamycin Complex 2 regulates actin polarization and endocytosis via multiple pathways. *J. Biol. Chem.* **290**, 14963-14978.

33. Goode, B. L., Eskin, J. A., and Wendland, B. (2015) Actin and endocytosis in budding yeast. *Genetics* **199**, 315-358.
34. Smythe, E., and Ayscough, K. R. (2003) The Ark1/Prk1 family of protein kinases. Regulators of endocytosis and the actin skeleton. *EMBO Rep.* **4**, 246-251.
35. Sherman, F., Fink, G. R., and Hicks, J. B. (1986) *Laboratory Course Manual for Methods in Yeast Genetics.*, Cold Spring Harbor Laboratory Press,. Cold Spring Harbor, NY.
36. Sambrook, J., and Russell, D. W. (2001) *Molecular Cloning: A Laboratory Manual*, 3rd ed., Cold Spring Harbor Laboratory Press, Cold Spring Harbor, NY
37. Baum, P., Thorner, J., and Honig, L. (1978) Identification of tubulin from the yeast *Saccharomyces cerevisiae*. *Proc. Natl. Acad. Sci. USA* **75**, 4962-4966.
38. Tsien, R. Y. (1998) The green fluorescent protein. *Annu. Rev. Biochem.* **67**, 509-544.
39. Shaner, N. C., Campbell, R. E., Steinbach, P. A., Giepmans, B. N., Palmer, A. E., and Tsien, R. Y. (2004) Improved monomeric red, orange and yellow fluorescent proteins derived from Discosoma sp. red fluorescent protein. *Nat. Biotechnol.* **22**, 1567-1572.
40. Edelstein, A., Amodaj, N., Hoover, K., Vale, R., and Stuurman, N. (2010) Computer control of microscopes using μManager. in *Curr. Protoc. Mol. Biol.* pp Unit 14.20
41. Collins, T. J. (2007) ImageJ for microscopy. *Biotechniques* **43** (Suppl), 25-30.
42. Sun, Y., Leong, N. T., Wong, T., and Drubin, D. G. (2015) A Pan1/End3/Sla1 complex links Arp2/3-mediated actin assembly to sites of clathrin-mediated endocytosis. *Mol. Biol. Cell* **26**, 3841-3856
43. Mok, J., Kim, P. M., Lam, H. Y., Piccirillo, S., Zhou, X., Jeschke, G. R., Sheridan, D. L., Parker, S. A., Desai, V., Jwa, M., Cameroni, E., Niu, H., Good, M., Remenyi, A., Ma, J. L., Sheu, Y. J., Sassi, H. E., Sopko, R., Chan, C. S., De Virgilio, C., Hollingsworth, N. M., Lim, W. A., Stern, D. F., Stillman, B., Andrews, B. J., Gerstein, M. B., Snyder, M., and Turk, B. E. (2010) Deciphering protein kinase specificity through large-scale analysis of yeast phosphorylation site motifs. *Sci. Signal.* **3**, ra12.1—ra12.13.
44. Iwamoto, K., Hayakawa, T., Murate, M., Makino, A., Ito, K., Fujisawa, T., and Kobayashi, T. (2007) Curvature-dependent recognition of ethanolamine phospholipids by duramycin and cinnamycin. *Biophys. J.* **93**, 1608-1619.
45. Kinoshita, E., Kinoshita-Kikuta, E., and Koike, T. (2015) Advances in Phos-tag-based methodologies for separation and detection of the phosphoproteome. *Biochim. Biophys. Acta* **1854**, 601-608.
46. Gaubitz, C., Oliveira, T. M., Prouteau, M., Leitner, A., Karuppasamy, M., Konstantinidou, G., Rispal, D., Eltschinger, S., Robinso, G. C., Thore, S., Aebersold, R., Schaffitzel, C.,

and Loewith, R. (2015) Molecular basis of the rapamycin insensitivity of Target of Rapamycin Complex 2. *Mol. Cell* **58**, 977-988.

47. Miyake, Y., Kozutsumi, Y., Nakamura, S., Fujita, T., and Kawasaki, T. (1995) Serine palmitoyltransferase is the primary target of a sphingosine-like immunosuppressant, ISP-1/myriocin. *Biochem. Biophys. Res. Commun.* **211**, 396-403.

48. Lu, R., Drubin, D. G., and Sun, Y. (2016) Clathrin-mediated endocytosis in budding yeast at a glance. *J. Cell Sci.* **129**, 1531-1536.

49. Zeng, G., Yu, X., and Cai, M. (2001) Regulation of yeast actin cytoskeleton-regulatory complex Pan1p/Sla1p/End3p by serine/threonine kinase Prk1p. *Mol. Biol. Cell* **12**, 3759-3772.

50. Ayscough, K. R. (2005) Coupling actin dynamics to the endocytic process in *Saccharomyces cerevisiae. Protoplasma* **226**, 81-88.

51. Takahashi, T., Furucht, T., and Naganuma, A. (2006) Endocytic Ark/Prk kinases play a critical role in adriamycin resistance in both yeast and mammalian cells. *Cancer Res.* **66**, 11932-11937.

52. Jin, M., and Cai, M. (2008) A novel function of Arp2p in mediating Prk1p-specific regulation of actin and endocytosis in yeast. *Mol. Biol. Cell* **19**, 297-307.

53. Huang, B., and Cai, M. (2007) Pan1p: an actin director of endocytosis in yeast. *Int. J. Biochem. Cell Biol.* **39**, 1760-1764.

54. Watson, H. A., Cope, M. J., Groen, A. C., Drubin, D. G., and Wendland, B. (2001) *In vivo* role for actin-regulating kinases in endocytosis and yeast epsin phosphorylation. *Mol. Biol. Cell* **12**, 3668-3679.

55. Sen, A., Madhivanan, K., Mukherjee, D., and Aguilar, R. C. (2012) The epsin protein family: coordinators of endocytosis and signaling. *Biomol. Concepts* **3**, 117-126.

56. Wendland, B., Steece, K. E., and Emr, S. D. (1999) Yeast epsins contain an essential N-terminal ENTH domain, bind clathrin and are required for endocytosis. *EMBO J.* **18**, 4383-4393.

57. Dores, M. R., Schnell, J. D., Maldonado-Baez, L., Wendland, B., and Hicke, L. (2010) The function of yeast epsin and Ede1 ubiquitin-binding domains during receptor internalization. *Traffic* **11**, 151-160.

58. Costakes, G. T., Sen, A., Aguilar, R. C., and Stauffacher, C. V. (2013) Crystallographic analysis of the ENTH domain from yeast epsin Ent2 that induces a cell division phenotype. *Protein Sci.* **22**, 755-761.

59. Huang, B., Zeng, G., Ng, A. Y., and Cai, M. (2003) Identification of novel recognition motifs and regulatory targets for the yeast actin-regulating kinase Prk1p. *Mol. Biol. Cell* **14**, 4871-4884.
60. Holtzman, D. A., Yang, S., and Drubin, D. G. (1993) Synthetic-lethal interactions identify two novel genes, *SLA1* and *SLA2*, that control membrane cytoskeleton assembly in *Saccharomyces cerevisiae*. *J. Cell Biol.* **122**, 635-644.
61. Warren, D. T., Andrews, P. D., Gourlay, C. W., and Ayscough, K. R. (2002) Sla1p couples the yeast endocytic machinery to proteins regulating actin dynamics. *J. Cell Sci.* **115**, 1703-1715.
62. Zeng, G., and Cai, M. (1999) Regulation of the actin cytoskeleton organization in yeast by a novel serine/threonine kinase Prk1p. *J. Cell Biol.* **144**, 71-82.
63. Henry, K. R., D'Hondt.K., Chang, J. S., Nix, D. A., Cope, M. J., Chan, C. S., Drubin, D. G., and Lemmon, S. K. (2003) The actin-regulating kinase Prk1p negatively regulates Scd5p, a suppressor of clathrin deficiency, in actin organization and endocytosis. *Curr. Biol.* **13**, 1564-1569.
64. Wiederkehr, A., Meier, K. D., and Riezman, H. (2001) Identification and characterization of *Saccharomyces cerevisiae* mutants defective in fluid-phase endocytosis. *Yeast* **18**, 759-773.
65. Martin, A. C., Xu, X. P., Rouiller, I., Kaksonen, M., Sun, Y., Belmont, L., Volkmann, N., Hanein, D., Welch, M., and Drubin, D. G. (2005) Effects of Arp2 and Arp3 nucleotide-binding pocket mutations on Arp2/3 complex function. *J. Cell Biol.* **168**, 315-328.
66. Farrell, K. B., Grossman, C., and Di Pietro, S. M. (2015) New regulators of clathrin-mediated endocytosis identified in Saccharomyces cerevisiae by systematic quantitative fluorescence microscopy. *Genetics* **201**, 1061-1070.
67. Cope, M. J., Yang, S., Shang, C., and Drubin, D. G. (1999) Novel protein kinases Ark1p and Prk1p associate with and regulate the cortical actin cytoskeleton in budding yeast. *J. Cell Biol.* **144**, 1203-1218.
68. Böttcher, C., Wicky, S., Schwarz, H., and Singer-Krüger, B. (2006) Sjl2p is specifically involved in early steps of endocytosis intimately linked to actin dynamics via the Ark1p/Prk1p kinases. *FEBS Lett.* **580**, 633-641.
69. Sekiya-Kawasaki, M., Groen, A. C., Cope, M. J., Kaksonen, M., Watson, H. A., Zhang, C., Shokat, K. M., Wendland, B., McDonald, K. L., McCaffery, J. M., and Drubin, D. G. (2003) Dynamic phosphoregulation of the cortical actin cytoskeleton and endocytic machinery revealed by real-time chemical genetic analysis. *J. Cell Biol.* **162**, 765-772.

70. Westmoreland, T. J., Wickramasekara, S. M., Guo, A. Y., Selim, A. L., Winsor, T. S., Greenleaf.A.L., Blackwell, K. L., Olson, J. A. J., Marks, J. R., and Bennett, C. B. (2009) Comparative genome-wide screening identifies a conserved doxorubicin repair network that is diploid specific in *Saccharomyces cerevisiae*. *PLoS One* **4**, e5830.1-e5830.20.
71. Demir, A. B., and Koc, A. (2015) High-copy overexpression screening reveals *PDR5* as the main doxorubicin resistance gene in yeast. *PLoS One* **10**, e0145108.1-e0145108.15.
72. Yamane-Sando, Y., Shimobayashi, E., Shimobayashi, M., Kozutsumi, Y., Oka, S., and Takematsu, H. (2014) Fpk1/2 kinases regulate cellular sphingoid long-chain base abundance and alter cellular resistance to LCB elevation or depletion. *MicrobiologyOpen* **3**, 196-212.
73. Dephoure, N., Gould, K. L., Gygi, S. P., and Kellogg, D. R. (2013) Mapping and analysis of phosphorylation sites: a quick guide for cell biologists. *Mol. Biol. Cell* **24**, 535-542.
74. Kallay, L. M., Brett, C. L., Tukaye, D. N., Wemmer, M. A., A., C., Odorizzi, G., and Rao, R. (2011) Endosomal Na+ (K+)/H+ exchanger Nhx1/Vps44 functions independently and downstream of multivesicular body formation. *J. Biol. Chem.* **286**, 44067-44077.
75. Sopko, R., Huang, D., Preston, N., Chua, G., Papp, B., Kafadar, K., Snyder, M., Oliver, S. G., Cyert., M., Hughes, T. R., Boone, C., and Andrews, B. (2006) Mapping pathways and phenotypes by systematic gene overexpression. *Mol. Cell* **21**, 319-330.
76. Holt, L. J., Tuch, B. B., Villen, J., Johnson, A. D., Gygi, S. P., and Morgan, D. O. (2009) Global analysis of Cdk1 substrate phosphorylation sites provides insights into evolution. *Science* **325**, 1682-1686
77. Fröhlich, F., Olson, D. K., Christiano, R., Farese, R. V. J., and Walther, T. C. (2016) Proteomic and phosphoproteomic analyses of yeast reveal the global cellular response to sphingolipid depletion. *Proteomics* **16**, 2759-2763.
78. Toshima, J., Y., Furuya, E., Nagano, M., Kanno, C., Sakamoto, Y., Ebihara, M., Siekhaus, D. E., and Toshima, J. (2016) Yeast Eps15-like endocytic protein Pan1p regulates the interaction between endocytic vesicles, endosomes and the actin cytoskeleton. *Elife* **5**, e10276.1-e10276.21.
79. Souza, C. M., and Pichler, H. (2007) Lipid requirements for endocytosis in yeast. *Biochim. Biophys. Acta* **1771**, 442-454.
80. Hannich, J. T., Umebayashi, K., and Riezman, H. (2011) Distribution and functions of sterols and sphingolipids. *Cold Spring Harb. Perspect. Biol.* **3**, a004762.1-a004762.14.

81. Fröhlich, F., Petit , C., Kory, N., Christiano, R., Hannibal-Bach, H. K., Graham, M., Liu, X., Ejsing, C. S., Farese, R. V. J., and Walther, T. C. (2015) The GARP complex is required for cellular sphingolipid homeostasis. *Elife* **4**, e08712.1-e08712.21.
82. Nagiec, M. M., Skrzypek, M., Nagiec, E. E., Lester, R. L., and Dickson, R. C. (1998) The LCB4 (YOR171c) and LCB5 (YLR260w) genes of Saccharomyces encode sphingoid long chain base kinases. *J. Biol. Chem.* **273**, 19437-19442.
83. Jandrositz, A., Turnowsky, F., and Högenauer, G. (1991) The gene encoding squalene epoxidase from *Saccharomyces cerevisiae*: cloning and characterization. *Genetics* **107**, 155-160.
84. Cole, S. P., and Deeley, R. G. (1998) Multidrug resistance mediated by the ATP-binding cassette transporter protein MRP. *Bioessays* **20**, 931-940.
85. Ueda, K., Clark, D. P., Chen, C. J., Roninson, I. B., Gottesman, M. M., and Pastan, I. (1987) The human multidrug resistance (mdr1) gene. cDNA cloning and transcription initiation. *J. Biol. Chem.* **262**, 505-508.
86. Meijer, C., Mulder, N. H., and de Vries, E. G. (1990) The role of detoxifying systems in resistance of tumor cells to cisplatin and adriamycin. *Cancer Treat Rev.* **17**, 389-407.
87. Cox, J., and Weinman, S. (2016) Mechanisms of doxorubicin resistance in hepatocellular carcinoma. *Hepat. Oncol.* **3**, 57-59.
88. Han, S., Lone, M. A., Schneiter, R., and Chang, A. (2010) Orm1 and Orm2 are conserved endoplasmic reticulum membrane proteins regulating lipid homeostasis and protein quality control. *Proc. Natl. Acad. Sci. USA* **107**, 5851-5856.
89. Brown, J. A., Sherlock, G., Myers, C. L., Burrows, N. M., Deng, C., Wu, H. I., McCann, K. E., Troyanskaya, O. G., and Brown, J. M. (2006) Global analysis of gene function in yeast by quantitative phenotypic profiling. *Mol. Syst. Biol.* **2**, 2006.0001.1—2006.0001.9.
90. Pomorski, T., Lombardi, R., Riezman, H., Devaux, P. F., van Meer, G., and Holthuis, J. C. (2003) Drs2p-related P-type ATPases Dnf1p and Dnf2p are required for phospholipid translocation across the yeast plasma membrane and serve a role in endocytosis. *Mol. Biol. Cell* **14**, 1240-1254.
91. Kolaczkowski, M., van der Rest, M., Cybularz-Kolaczkowska, A., Soumillion, J. P., Konings, W. N., and Goffeau, A. (1996) Anticancer drugs, ionophoric peptides, and steroids as substrates of the yeast multidrug transporter Pdr5p. *J. Biol. Chem.* **271**, 31543-31548.

92. Rogers, B., Decottignies, A., Kolaczkowski, M., Carvajal, E., Balzi, E., and Goffeau, A. (2001) The pleitropic drug ABC transporters from *Saccharomyces cerevisiae*. *J. Mol. Microbiol. Biotechnol.* **3**, 207-214.
93. Golin, J., Ambudkar, S. V., Gottesman, M. M., Habib, A. D., Sczepanski, J., Ziccardi, W., and May, L. (2003) Studies with novel Pdr5p substrates demonstrate a strong size dependence for xenobiotic efflux. *J. Biol. Chem.* **278**, 5963-5969.
94. Decottignies, A., Lambert, L., Catty, P., Degand, H., Epping, E. A., Moye-Rowley, W. S., Balzi, E., and Goffeau, A. (1995) Identification and characterization of SNQ2, a new multidrug ATP binding cassette transporter of the yeast plasma membrane. *J. Biol. Chem.* **270**, 18150-18157.
95. Kihara, A., and Ilgarashi, Y. (2004) Cross talk between sphingolipids and glycerophospholipids in the establishment of plasma membrane asymmetry. *Mol. Biol. Cell* **15**, 4949-4959.
96. Johnson, S. S., Hanson, P. K., Manoharlal, R., Brice, S. E., Cowart, L. A., and Moye-Rowley, W. S. (2010) Regulation of yeast nutrient permease endocytosis by ATP-binding cassette transporters and a seven-transmembrane protein, RSB1. *J. Biol. Chem.* **285**, 35792-35802.
97. Khakhina, S., Johnson, S. S., Manoharlal, R., Russo, S. B., Blugeon, C., Lemoine, S., Sunshine, A. B., Dunham, M. J., Cowart , L. A., Devaux, F., and Moye-Rowley, W. S. (2015) Control of plasma membrane permeability by ABC transporters. *Eukaryot. Cell* **14**, 442-453.
98. Hua, Z., Fatheddin, P., and Graham, T. R. (2002) An essential subfamily of Drs2p-related P-type ATPases is required for protein trafficking between Golgi complex and endosomal/vacuolar system. *Mol. Biol. Cell* **13**, 3162-3177.
99. Kaksonen, M., Toret, C. P., and Drubin, D. G. (2005) A modular design for the clathrin- and actin-mediated endocytosis machinery. *Cell* **123**, 305-320.
100. Carminati, J. L., and Stearns, T. (1997) Microtubules orient the mitotic spindle in yeast through dynein-dependent interactions with the cell cortex. *J. Cell Biol.* **138**, 629-641.
101. Sikorski, R. S., and Hieter, P. (1989) A system of shuttle vectors and yeast host strains designed for efficient manipulation of DNA in *Saccharomyces cerevisiae*. *Genetics* **122**, 19-27
102. Bardwell, L., Cook, J. G., Zhu-Shimoni, J. X., Voora, D., and Thorner, J. (1998) ifferential regulation of transcription: repression by unactivated mitogen-activated protein kinase Kss1 requires the Dig1 and Dig2 proteins. *Proc. Natl. Acad. Sci. USA* **95**, 15400-15405.

103. Smolka, M. B., Albuquerque, C. P., Chen, S. H., and Zhou, H. (2007) Proteome-wide identification of in vivo targets of DNA damage checkpoint kinases. *Proc. Natl. Acad. Sci. USA* **104**, 10364-10369
104. Albuquerque, C. P., Smolka, M. B., Payne, S. H., Bafna, V., Eng, J., and Zhou, H. (2008) A multidimensional chromatography technology for in-depth phosphoproteome analysis. *Mol. Cell. Proteomics* **7**, 1389-1396
105. Huber, A., Bodenmiller, B., Uotila, A., Stahl, M., Wanka, S., Gerrits, B., Aebersold, R., and Loewith, R. (2009) Characterization of the rapamycin-sensitive phosphoproteome reveals that Sch9 is a central coordinator of protein synthesis. *Genes Dev.* **23**, 1929-1943.
106. Bodenmiller, B., Wanka, S., Kraft, C., Urban, J., Campbell, D., Pedrioli, P. G., B., G., Picotti, P., Lam, H., Vitek, O., Brusniak, M. Y., Roschitzki, B., Zhang, C., Shokat, K. M., Schlapbach, R., Colman-Lerner, A., Nolan, G. P., Nesvizhskii, A. I., Peter, M., Loewith, R., von Mering, C., and Aebersold, R. (2010) Phosphoproteomic analysis reveals interconnected system-wide responses to perturbations of kinases and phosphatases in yeast. *Sci. Signal.* **3**, rs4.1—rs4.8.
107. Swaney, D. L., Beltrao, P., Starita, L., Guo, A., Rush, J., Fields, S., Krogan, N. J., and Villén, J. (2013) Global analysis of phosphorylation and ubiquitylation cross-talk in protein degradation. *Nat Methods* **10**, 676-682.
108. Li, X., Gerber, S. A., Rudner, A. D., Beausoleil, S. A., Haas, W., Villén, J., Elias, J. E., and Gygi, S. P. (2007) Large-scale phosphorylation analysis of alpha-factor-arrested *Saccharomyces cerevisiae*. *J. Proteome Res.* **6**, 1190-1197.
109. Soulard, A., Cremonesi, A., Moes, S., Schütz, F., Jenö, P., and Hall, M. N. (2010) The rapamycin-sensitive phosphoproteome reveals that TOR controls protein kinase A toward some but not all substrates. *Mol. Biol. Cell* **21**, 3475-3486.
110. Chi, A., Huttenhower, C., Geer, L. Y., Coon, J. J., Syka, J. E., DL., B., Shabanowitz, J., Burke, D. J., Troyanskaya, O. G., and Hunt, D. F. (2007) Analysis of phosphorylation sites on proteins from *Saccharomyces cerevisiae* by electron transfer dissociation (ETD) mass spectrometry. *Proc. Natl. Acad. Sci. USA* **104**, 2193-2198.
111. Gnad, F., de Godoy, L. M., Cox, J., Neuhauser, N., Ren, S., Olsen, J. V., and Mann, M. (2009) High-accuracy identification and bioinformatic analysis of in vivo protein phosphorylation sites in yeast. *Proteomics* **9**, 4642-4652.

112. Soufi, B., Kelstrup, C. D., Stoehr, G., Fröhlich, F., Walther, T. C., and Olsen, J. V. (2009) Global analysis of the yeast osmotic stress response by quantitative proteomics. *Mol. Biosyst.* **5**, 1337-1346.
113. Gruhler, A., Olsen, J. V., Mohammed, S., Mortensen, P., Faergeman, N. J., Mann, M., and Jensen, O. N. (2005) Quantitative phosphoproteomics applied to the yeast pheromone signaling pathway. *Mol. Cell. Proteomics* **4**, 310-327.

973 **Table 1.** *S. cerevisiae* strains used in this study.

Strain	Genotype	Source/Reference
BY4741	*MAT***a** *his3*Δ*1 leu2*Δ*0 met15*Δ*0 ura3*Δ*0*	Research Genetics, Inc.
YFR205	BY4741 *fpk1*Δ*::*KanMX4 *fpk2*Δ*::*KanMX4 *lys2*Δ*0*	(23)
YJW2	BY4741 Fpk1^{11A}::*HIS3*	(23)
YFR437	BY4741 Akl1-mCherry::*CaURA3*	This study
YFR468	BY4741 Fpk1^{11A}::*HIS3* Akl1-mCherry::*CaURA3*	This study
YFR469	BY4741 *fpk1*Δ*::*KanMX4 *fpk2*Δ*::*KanMX4 Akl1-mCherry::*CaURA3*	This study
YFR515	BY4741 Akl1-mCherry::*CaURA3* Sla1-GFP::*HIS3*	This study
PFY3272C	BY4741 *dnf1*Δ*::*KanMX4 *dnf2*Δ*::*KanMX4 *dnf3*Δ*::*KanMX4	(98)
*ypk1*Δ	BY4741 *ypk1*Δ::KanMX4	Research Genetics, Inc.
yKL28	BY4741 *slm1*Δ::KanMX *slm2*Δ::KanMX [pRS416-Ypk1(D242A)-3HA]	This study
GFY1770	BY4741 *DNF1::*HygMX *dnf2*Δ::KanMX *dnf3*Δ*::*KanMX	This study
GFY1773	BY4741 *DNF1-GFP::*HygMX *dnf2*Δ*::*KanMX *dnf3*Δ*::*KanMX	This study
GFY1772	BY4741 *DNF1(S348A S358A S365A S1526A S1545A S1552A)::*HygMX *dnf2*Δ*::*KanMX *dnf3*Δ*::*KanMX	This study
GFY1775	BY4741 *DNF1(S348A S358A S365A S1526A S1545A S1552A)-GFP::*HygMX *dnf2*Δ*::*KanMX *dnf3*Δ*::*KanMX	This study
GFY1728	BY4741 *dnf1*Δ*::*natNT2 *dnf2*Δ*::*KanMX *dnf3*Δ*::*KanMX	This study
BY4742	*MAT*α *his3*Δ*1 leu2*Δ*0 lys2*Δ*0 ura3*Δ*0*	Research Genetics, Inc.
*ypk2*Δ	BY4742 *ypk2*Δ::KanMX4	Research Genetics, Inc.
YFR381	BY4742 *slm1*Δ*::*KanMX4 *slm2*Δ*::*KanMX4 [pRS315-Ypk1(D242A)-Myc]	This study
JTY6532	BY4742 *akl1*Δ*::*KanMX	Research Genetics, Inc.
YFR474-A	BY4742 Akl1-3xFLAG::*URA3*	Research Genetics, Inc.
YFR475-A	BY4742 Akl1(S960A S1072A)-3xFLAG::*URA3*	This study
YFR476-A	BY4742 Akl1(S960E S1072E)-3xFLAG::*URA3*	This study
YFR479	BY4742 *akl1*Δ::Hyg^{r}	This study
*avo3*ΔCT *TOR1-1*	*MAT***a** *avo3*Δ1274-1430 *TOR1-1 trp1 his3 ura3 leu2 rme1* (TB50 strain background)	(46)
YFR491-A	*MAT***a** *ENT2-GFP::HIS3 his3 leu2 ura3 met15*	This study

YFR492-A	*MAT***a** *ENT2-GFP::HIS3 fpk1*Δ*::*KanMX4 *fpk2*Δ*::*KanMX4 *his3 leu2 ura3 lys2*	This study
JTY5180	*MAT*α *ABP1-RFP::HIS3 his3-Δ200 ura3-52 leu2-3,112* (DDY3058)	(99)
YFR507	*MAT***a** Akl1::*URA3 Sla1-GFP::CgHIS Abp1-RFP::HIS3 his3-Δ200 ura3-52 leu2-3,112 lys2-801*	This study
YFR508	*MAT***a** Akl1(S960A S1072A)::*URA3 Sla1-GFP::CgHIS Abp1-RFP::HIS3 his3-Δ200 ura3-52 leu2-3,112 lys2-801*	This study

974

975

976

977

978

979 **Table 2**. Plasmids used in this study.

Plasmid	Description	Source/Reference
pGEX4T-1	GST tag, bacterial expression vector	GE Healthcare, Inc.
pAX15	pGEX4T-1 Fpk1-GSGSHHHHHH	This study
pJY10	pGEX4T-1 Fpk1(D621A)-GSGSHHHHHH	This study
pFR290	pGEX4T-1 Akl1(767-1108)	This study
pFR293	pGEX4T-1 Akl1(767-1108; S960A)	This study
pFR294	pGEX4T-1 Akl1(767-1108; S1072A)	This study
pFR297	pGEX4T-1 Akl1(767-1108; S960A S1072A)	This study
pGEX3	GST tag, bacterial expression vector	GE Healthcare, Inc.
pDD0214	pGEX3 Sla1(854-918)	Drubin lab, UC Berkeley
pTS408	*CEN URA3, GAL1*$_{prom}$ GFP vector	(100)
pDD0938	pTS408 GFP-Akl1	Drubin lab, UC Berkeley
pFR303	pTS408 GFP-Akl1(S960A S1072A)	This study
pKL31	pTS408 GFP-Akl1(D181A S960A S1072A)	This study
pFR304	pTS408 GFP-Akl1(Δ30-751)	This study
pFR329	pTS408 GFP-Akl1(Δ30-751; S960A)	This study
pFR328	pTS408 GFP-Akl1(Δ30-751; S1072A)	This study
pFR334	pTS408 GFP-Akl1(Δ30-751; S960A S1072A)	This study
pRS315	*CEN LEU2*	(101)
pFR234	pRS315 Ypk1(D242A)-Myc	This study
pFR316	pRS315 Akl1-3xFLAG	This study
pFR318	pRS315 Akl1(D181Y)-3xFLAG	This study
pFR319	pRS315 Akl1(S960A S1072A)-3xFLAG	This study

YCpLG	*CEN*, *LEU2*, $GAL1_{prom}$ vector	(102)
pFR360	YCpLG 3xFLAG-Sla1(851-1244)	This study
pRS416	*CEN*, *URA3* vector	(101)
pPL215	pRS416 $MET25_{prom}$ Ypk1-3xHA	(9)
pKL27	pRS416 $MET25_{prom}$ Ypk1(D242A)-3xHA	This study

980

981

982

983

984

985 **Table 3**. *S. cerevisiae* proteins containing at least two Fpk1 phospho-acceptor site motifs.
986

Protein/ORF	Function	Fpk1 motifs	Evidence for phosphorylation *in vivo*
Dnf1/YER166W	Aminoglycerophospholipid translocase (flippase)	RSS^{348}LD RVS^{358}AD RPS^{365}LD RSS^{1526}LD RYS^{1545}VE RTS^{1552}LD	(23,76,103-107)
Dnf2/YDR093W	Aminoglycerophospholipid translocase (flippase)	RGS^{386}LD RMS^{396}AD RPS^{403}LD RTS^{1566}LD RAS^{1592}LD	(23,32,76,103-109)
Dnf3/YMR162C	Aminoglycerophospholipid translocase (flippase)	RPS^{651}LD RNS^{661}IE RKS^{88}LE RIS^{973}ID	(76,107,110-112)
Ypk1/YKL126W	Ser/Thr protein kinase controlling PM lipid and protein homeostasis	RSS^{51}LD RVS^{71}YD	(23,72,107)
Akl1/YBR059C	Ser/Thr protein kinase; (member, with Ark1 and Prk1, of a protein kinase family involved in control of endocytosis and actin cytoskeleton organization)	RQS^{960}LD RQS^{1072}LD	(32,76,103,105-109); this study
Cti6/ YPL181W	PHD domain-containing component of the Rpd3L histone deacetylase complex	RNS^{216}MD RRS^{406}AD	(32,76,103,104,106,108,109)
Dit2/YDR402C	N-formyltyrosine oxidase	RES^{62}ME RWS^{459}LD	—
Ent4/YLL038C	Protein of unknown function (contains an N-terminal epsin-like domain)	RQS^{182}LE RFS^{213}LD	(76,106,107,109)
Erg1/YGR175C	Squalene mono-oxygenase	RPS^{302}FD RKS^{386}ID	—
Ira2/YOL081W	GTPase-activating protein (GAP) for Ras1 and Ras2 (paralog of Ira1)	RAS^{547}YD RLS^{779}ID	—
Irc20/YLR247C	E3 ubiquitin ligase and putative helicase	RKS^{152}LE RFS^{224}VE RES^{298}VE	—
Lcb5/YLR260w	Long-chain (sphingoid) base kinase (paralog of Lcb4)	RSS^{55}ID RCS^{302}IE	(76,103,107,109)

Mks1/YNL076W	Negative transcriptional regulator [with pleiotropic roles in lysine biosynthetic pathway and nitrogen regulation, and in both Ras-cAMP and retrograde (RTG) mitochondria-to-nucleus signaling]	RLS^{453}MD RQS^{518}MD	(32,76,105-107,109)
Not3/YIL038C	Subunit of CCR4-NOT global transcriptional regulator	RRS^{83}VE RSS^{348}AD	—
Pfa3/YNL326C	Palmitoyl-CoA transferase of the DHHC-CRD family required C-terminal S-palmitoylation of vacuolar membrane protein Vac8	RPS^{322}LE RAS^{329}VE	(76,107)
Pkh3/YDR466W	Protein kinase (weak similarity to Pkh1 and Pkh2 and mammalian PDK1)	RIS^{283}LE RNS^{499}ID	—
Prp2/YNR011C	RNA-dependent DExD/H-box ATPase required for spliceosome activation	RAS^{545}VD RKS^{619}LE	—
Tus1/YLR425W	Guanine nucleotide exchange factor (GEF) for Rho1	RKS^{27}IE RPS^{1163}IE	(106,107,111,112)
Vps54/YDR027C	Component of the Golgi-associated retrograde protein (GARP) complex	RLS^{69}LD RRS^{78}FD	(76,103,104,107-109,113)
Yta6/YPL074W	Cortically-localized putative AAA+ ATPase of the Cdc48/Pas1/Sec18 sub-family	RAS^{255}LD RRS^{278}LD RKS^{296}ME	(32,76,103-106,109)

987

988

FIGURE LEGENDS

FIG. 1. Absence of Fpk1 phosphorylation impairs PtdEth flipping by Dnf1. (A) Strains *DNF1 dnf2*Δ *dnf3*Δ (GFY1770), *DNF1-GFP dnf2*Δ *dnf3*Δ (GFY1773), *DNF1*^{6A} *dnf2*Δ *dnf3*Δ (GFY1772), *DNF1*^{6A}*-GFP dnf2*Δ *dnf3*Δ (GFY1775), and *dnf1*Δ *dnf2*Δ *dnf3*Δ (GFY1728) were plated as a lawn on YPD plates and 10 µl of stock solution of duramycin (either 8 mM or 4 mM) were spotted onto sterile filter paper disks which were immediately placed onto the lawn. Plates were scanned after incubation at 30˚C for 2 days. (B) Extracts from *dnf1*Δ *dnf2*Δ *dnf3*Δ (GFY1728), *DNF1-GFP dnf2*Δ *dnf3*Δ (GFY1773), and *DNF1*^{6A}*-GFP dnf2*Δ *dnf3*Δ (GFY1775) cells were resolved by SDS-PAGE and analyzed by immunoblotting with anti-GFP antibodies. (C) The same cells as in (B), co-stained with CellMask Orange™ to highlight the plasma membrane, were viewed by fluorescence microscopy as described in Materials and Methods.

FIG. 2. Fpk1 phosphorylates Akl1 at S960 and S1072. (A) Schematic representation of the Akl1, Ark1 and Prk1 protein kinases. The catalytic domain (red rectangle) is near the amino terminus. Akl1 has the longest C-terminal segment and only Akl1 contains consensus Fpk1 phospho-acceptor site motifs, both near its C-terminus. (B) GST-Fpk1 (pAX15, WT) or catalytically inactive ("kinase dead", KD) mutant GST-Fpk1(D621A) (pJY10) were purified from *E. coli*, incubated with [γ–^{32}P]ATP and either GST-Akl1(767-1108) (pFR290), GST-Akl1(767-1108; S960A) (pFR293), GST-Akl1(767-1108; S1072A) (pFR294), or GST-Akl1(767-1108; S960A S1072A) (pFR297) also purified from *E. coli*. Resulting products were resolved by SDS-PAGE and analyzed by autoradiography and staining with Coomassie dye. (C) A wild-type (WT) strain (BY4741) or an isogenic *fpk1*Δ *fpk2*Δ mutant (YFR205) expressing from the *GAL1* promoter either GFP-Akl1 (pDD0938) or GFP-Akl1(S960A S1072A) (pFR303) were grown to mid-exponential phase and lysed. The resulting extracts were resolved on a Phos-tag gel and analyzed by immunoblotting with anti-GFP antibodies. (D) Otherwise wild-type cells expressing full-length Akl1-mCherry from its endogenous promoter at its normal chromosomal locus

(YFR437) were grown, extracts prepared, treated with calf intestinal phosphatase, and then resolved and analyzed as in Fig. 2C. (E) As in (C) except that the strains were expressing GFP-Akl1 in which residues 30 to 751 were deleted (pFR304), or the same construct with the S960A (pFR329), S1072A (pFR328), or S960A S1072A mutations (pFR334). (F) A wild-type strain (BY4741) expressing GFP-Akl1(Δ30-751) (pFR304) was grown, extracts prepared, treated with calf intestinal phosphatase (CIP), and then resolved and analyzed as in Fig. 2E. (G) Strains BY4741 (WT) and *avo3*$^{\Delta CT}$ *TOR1-1* were transformed with GFP-Akl1(Δ30-751) (pFR304), grown to mid-exponential phase, untreated (-) or treated (+) with rapamycin (0.2 μM) for 10 min, which in this strain specifically inhibits TORC2, before being lysed and analyzed as in (C). (H) *avo3*$^{\Delta CT}$ *TOR1-1* cells transformed with GFP-Akl1(Δ30-751) (pFR304), GFP-Akl1(Δ30-751; S960A) (pFR329), GFP-Akl1(Δ30-751; S1072A) (pFR328), or GFP-Akl1(Δ30-751; S960A S1072A) (pFR334) were grown and analyzed, as in (G).

FIG. 3. Sphingolipids stimulate Fpk1 function by a mechanism distinct from alleviation of TORC2-Ypk1-mediated inhibition. (A) A wild-type (WT) strain (BY4741) or an isogenic *fpk1*Δ *fpk2*Δ mutant (YFR205) expressing from the *GAL1* promoter GFP-Akl1(pDD0938) were grown to mid-exponential phase, expression induced with galactose, and after one hour induction, treated with vector (-), 1.25 μM myriocin (Myr), or 10 μM phytosphingosine (PHS) for 2 additional hours. The cells were then lysed and analyzed as in Fig. 2E. (B) Same as in (A), except with strains BY4741 (WT), *slm1*Δ *slm2*Δ expressing Ypk1^{D242A} (YFR381), and *ypk1*Δ. (C) Anti-Ypk1 phospho-T662 antibodies recognize the TORC2-phosphorylated forms of endogenous Ypk1 and Ypk2, and plasmid-expressed Ypk1-3xHA. Wild-type (BY4741), or otherwise isogenic *ypk1Δ* or *ypk2Δ* cells expressing Ypk1-3xHA (pPL215) were grown to mid-exponential phase and then treated with either vehicle (methanol) or 1.25 μM myriocin for 2 h to induce TORC2 activation prior to harvesting. Whole-cell extracts were prepared, resolved by Phos-tag SDS-PAGE and analyzed by immunoblotting with anti-Ypk1 phospho-T662 antibodies

and anti-HA.11 epitope antibody. (D) Same as in (C) except that wild-type (BY4741) or *slm1Δ slm2Δ* (yKL28) cells expressing Ypk1(D242A)-3xHA (pKL27) were used.

FIG. 4. Phosphorylation by Fpk1 down-regulates Akl1 activity. (A) Sequence of Sla1. Consensus Akl1/Prk1 phospho-acceptor site (*yellow box*), matching either the Prk1 motif (**L/I/V/M**xxQ/N/T/Sx**TG**) determined in Pan1 (59) or the Akl1 motif (**L/I/V/M**xxQ/H/M/T/N/Ax**TG**) determined using synthetic peptide arrays (43). Consensus Ypk1 phospho-acceptor sites (*turquoise box*), **R**x**R**xx**S**[Φ] (where [Φ] is a preference for a hydrophobic amino acid) (8). (B) Cultures of an *akl1Δ* mutant (YFR479) expressing either Akl1-3xFLAG (pFR316) or a catalytically-inactive ("kinase dead", KD) mutant, Akl1(D181Y)-3xFLAG (pFR318), were lysed and the corresponding 3xFLAG-tagged proteins recovered by immunoprecipitation with mouse anti-FLAG antibodies. The resulting immunoprecipitates were incubated with [γ-^{32}P]ATP and GST-Sla1(854-918) that had been purified from *E. coli* harboring plasmid pDD0214. The resulting products were resolved by SDS-PAGE and analyzed, as described in Materials and Methods. (C) As in (B) except that an *akl1*Δ mutant (YFR479) expressing either Akl1-3xFLAG (pFR316) or Akl1^{AA}-3xFLAG (pFR319) were used. Numbers beneath each time point represent the autoradiogram/Coomassie signals, normalized to the ratio observed for WT Akl1 at 15 min. (D) The immunoprecipitates obtained in (C) were resolved on SDS-PAGE and analyze by immunoblotting with anti-FLAG antibodies. (E) A wild-type (WT) strain (BY4741) or an isogenic *fpk1*Δ *fpk2*Δ mutant (YFR205) (*left*), or strains Akl1 (YFR507) or Akl1^{AA} (YFR508) (*right*). expressing from the *GAL1* promoter 3xFLAG-Sla1(851-1244) (pFR360) were grown to mid-exponential phase and expression induced with galactose for 3 hours. The cells were harvested, lysed, trichloroacetic acid extracts prepared, and the precipitated proteins resolubilized, treated with calf intestinal phosphatase (CIP), resolved by SDS-PAGE, and analyzed by immunoblotting. (F) Strains Ent2-GFP (YFR491-A) and Ent2-GFP *fpk1*Δ *fpk2*Δ (YFR492-A) were grown to mid-exponential phase, cells harvested and lysed. The resulting

extracts were resolved in duplicate on a Phos-tag gel (rightmost pair of lanes were loaded with 25% more sample than the leftmost pair of lanes) and analyzed by immunoblotting with anti-GFP antibodies.

FIG. 5. Fpk1 phosphorylation does not affect the stability or localization of Akl1. (A) Extracts from Akl1-mCherry (YFR437), Fpk1^{11A} Akl1-mCherry (YFR468) [Fpk1^{11A} is hyperactive because no longer submitted to negative regulation by Gin4 (31)], and *fpk1*Δ *fpk2*Δ Akl1-mCherry (YFR469) cells were resolved by standard SDS-PAGE and analyzed by immunoblotting with anti-RFP antibodies. (B) Extracts from Akl1-3xFLAG (YFR474-A), Fpk1^{11A}-3xFLAG (YFR475-A), and Akl1^{EE}-3xFLAG (YFR476-A) cells were resolved by SDS-PAGE and analyzed by immunoblotting with anti-FLAG antibodies. (C) The same strains as in (A) were examined by fluorescence microscopy.

FIG. 6. Lack of negative regulation of Akl1 by Fpk1 impedes endocytosis. (A) Cultures of an *akl1Δ* strain (YFR479) containing either an empty vector (V; YCpUG) or expressing from the *GAL1* promoter in the same vector either GFP-Akl1^{AA} (pFR303) or a catalytically-inactive ("kinase dead", KD) derivative, GFP-Akl1^{AA}(D181A) (pKL31), were induced on galactose medium for 2.5 h, incubated with 4 mg/ml Lucifer Yellow CH (LY) for 30 min at 24°C, and then viewed directly by fluorescence microscopy. (B) Cells (YFR515) expressing both Akl1-mCherry and Sla1-GFP from their endogenous promoters at their normal chromosomal loci were grown on YPD and viewed by fluorescence microscopy. (C) Akl1 Sla1-GFP Abp1-RFP (WT, YFR507) and Akl1^{AA} Sla1-GFP Abp1-RFP (YFR508) strains were examined by fluorescence video microscopy (see Supplemental Movies 1 and 2) and kymographs were plotted, as described in Materials and Methods. (D) The mean Sla1-GFP lifetime at cell cortex was measured from multiple kymographs, as in (C). (E) The total number of Sla1-GFP patches per cell subsequently joined by Abp1-RFP and moved toward the cell center, a hallmark of actin-driven internalization (48), were counted in cells as in (C) [total number cells examined (n)].

FIG. 7. Fpk1 effects on both Akl1 and flippase function influence drug sensitivity. (A) Serial 10-fold dilutions of BY4741 (WT), *akl1*Δ (JTY6532), Fpk1^{11A} (YJW2), *fpk1*Δ *fpk2*Δ (YFR205), and *dnf1*Δ *dnf2*Δ *dnf3*Δ (PFY3272C) cells were spotted on plates lacking (-) or containing (+) doxorubicin (86 μM). The plates were scanned after incubation for 2 days at 30˚C. (B) Same as in (A), except with strains Akl1-3xFLAG (YFR474-A), Akl1^{AA}-3xFLAG (YFR475-A), and Akl1^{EE}-3xFLAG (YFR476-A) cells and a different stock of doxorubicin (which is light-sensitive) was used. (C) Serial 10-fold dilutions of *akl1*Δ (YFR479) cells carrying pRS315 (empty vector) or expressing from the same vector Akl1-3xFLAG (pFR316) or Akl1^{AA}-3xFLAG (pFR319) were spotted on plates lacking (-) or containing (+) hygromycin B (70 μM). The plates were scanned after incubation for 2 days at 30˚C. (D) Serial 10-fold dilutions of *akl1*Δ (YFR479) cells carrying YCpUG (empty vector) or expressing from the *GAL1* promoter GFP-Akl1 (pDD0938) or GFP-Akl1^{AA} (pFR303) were spotted on plates containing dextrose (Dex) or galactose (Gal), lacking (-) or containing 0.8 μM myriocin (+Myr) as indicated. The plates were scanned after incubation for 3 days at 30˚C.

FIG. 8. Fpk1 protein kinase is a signaling node that controls membrane permeability and the efficiency of endocytosis. In cells stressed by a diminution in the supply of sphingolipids, Fpk1 will be less active for two reasons: (i) lack of direct stimulation by MIPC (23); and, (ii) inhibitory phosphorylation by Ypk1, which is activated in a TORC2-dependent manner when sphingolipids are limiting (6,7). The cell cycle-regulated protein kinase Gin4 also inhibits Fpk1; thus, Fpk1 is also down-regulated when Gin4 is active (31). Fpk1, in turn, phosphorylates and stimulates the flippases Dnf1 and Dnf2 and, as shown in this study, phosphorylates and negatively regulates Akl1. One function of Akl1 is to impede endocytosis by phosphorylation of multiple endocytic factors (including Sla1, Ent2 and Pan1), which disables their function. Thus, when Fpk1 activity is high, Akl1 function is down-regulated and endocytosis can proceed; when Fpk1 activity is low,

Akl1 function is released from inhibition, causing phosphorylation of it targets, thereby down-modulating the efficiency of endocytosis. Two concomitant changes in PM composition ensue when Fpk1 activity is decreased: aminoglycerophospholipid content in the outer leaflet will remain higher due to lack of Fpk1-mediated stimulation of the flippases; and, bulk membrane and lipid internalization via clathrin-mediated endocytosis will be impeded. Both effects contribute to conferring elevated resistance to certain toxic xenobiotic compounds, such as doxorubicin and hygromycin B.

Figure 1

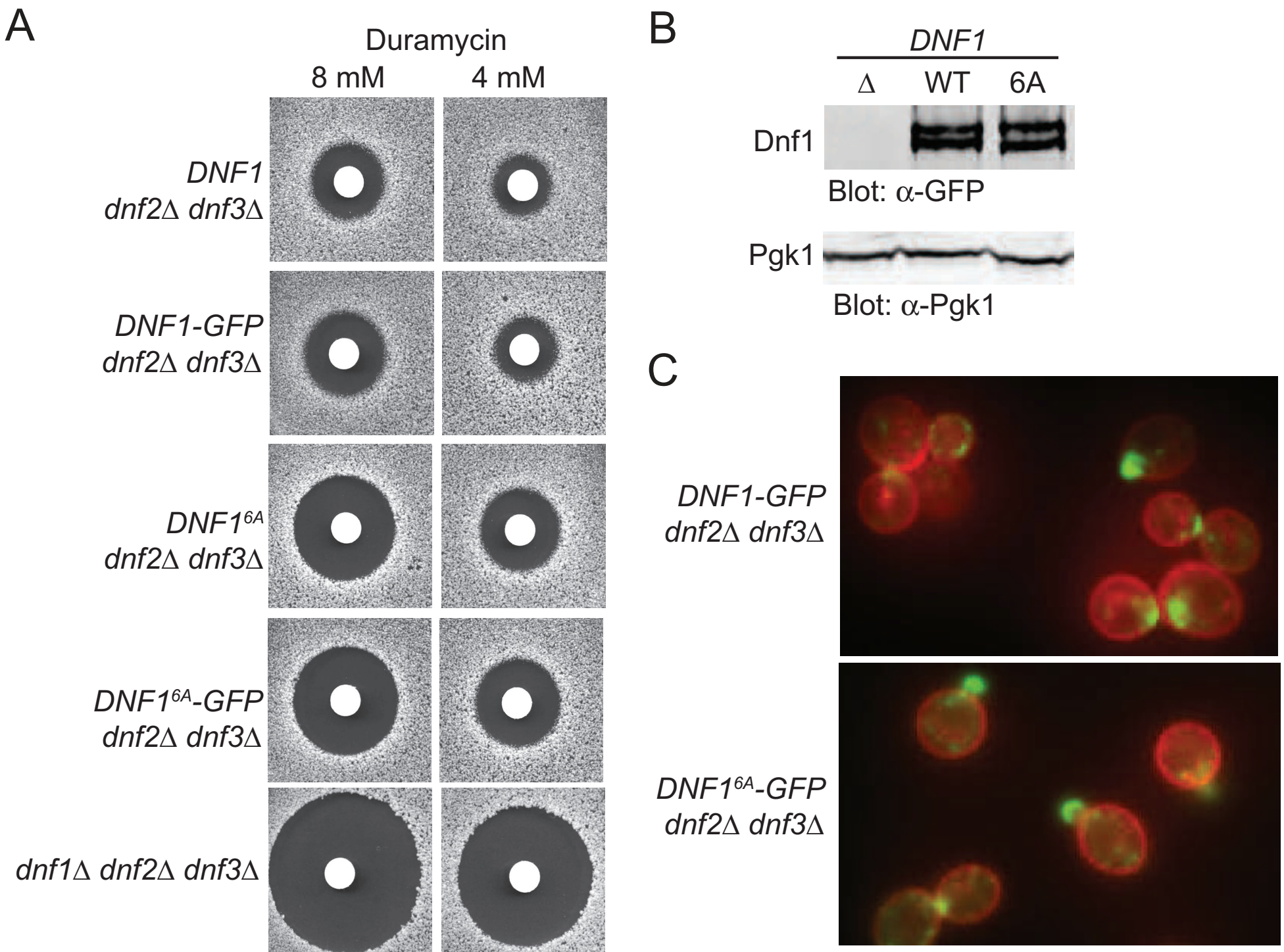
A
Duramycin
8 mM
4 mM
DNF1
dnf2Δ dnf3Δ
DNF1-GFP
dnf2Δ dnf3Δ
DNF1^6A
dnf2Δ dnf3Δ
DNF1^6A-GFP
dnf2Δ dnf3Δ
dnf1Δ dnf2Δ dnf3Δ
B
DNF1
Δ
WT
6A
Dnf1
Blot: α-GFP
Pgk1
Blot: α-Pgk1
C
DNF1-GFP
dnf2Δ dnf3Δ
DNF1^6A-GFP
dnf2Δ dnf3Δ

Figure 2

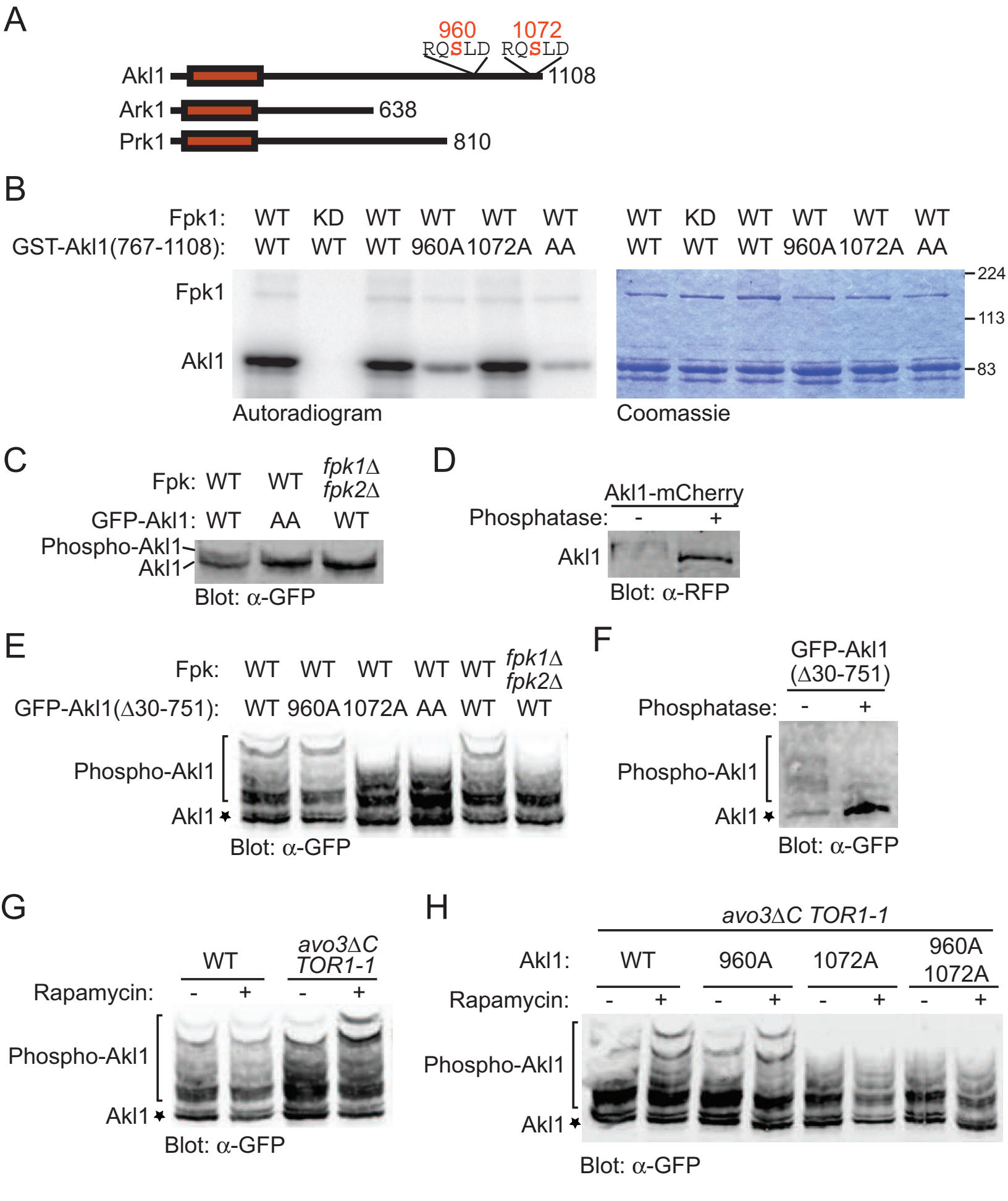
A
960
1072
RQSLD
RQSLD
Akl1
1108
Ark1
638
Prk1
810
B
Fpk1: WT KD WT WT WT WT
GST-Akl1(767-1108): WT WT WT 960A 1072A AA
WT KD WT WT WT WT
WT WT WT 960A 1072A AA
Fpk1
Akl1
224
113
83
Autoradiogram
Coomassie
C
Fpk: WT WT fpk1Δ fpk2Δ
GFP-Akl1: WT AA WT
Phospho-Akl1
Akl1
Blot: α-GFP
D
Akl1-mCherry
Phosphatase: - +
Akl1
Blot: α-RFP
E
Fpk: WT WT WT WT WT fpk1Δ fpk2Δ
GFP-Akl1(Δ30-751): WT 960A 1072A AA WT WT
Phospho-Akl1
Akl1
Blot: α-GFP
F
GFP-Akl1 (Δ30-751)
Phosphatase: - +
Phospho-Akl1
Akl1
Blot: α-GFP
G
WT
avo3ΔC TOR1-1
Rapamycin: - + - +
Phospho-Akl1
Akl1
Blot: α-GFP
H
avo3ΔC TOR1-1
Akl1: WT 960A 1072A 960A 1072A
Rapamycin: - + - + - + - +
Phospho-Akl1
Akl1
Blot: α-GFP

Figure 3

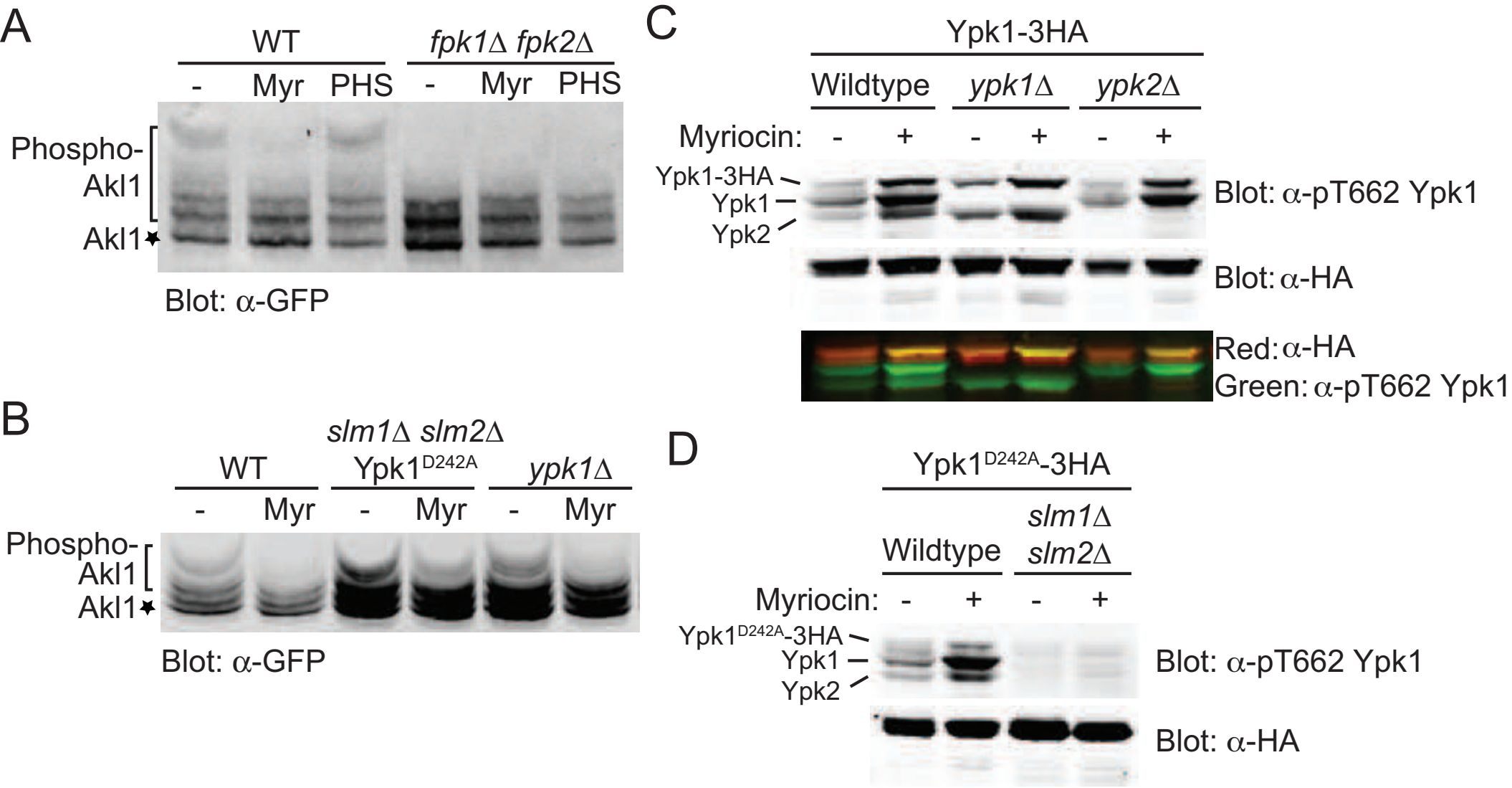
A
WT
fpk1Δ fpk2Δ
- Myr PHS - Myr PHS
Phospho-Akl1
Akl1
Blot: α-GFP
B
slm1Δ slm2Δ
WT
Ypk1D242A
ypk1Δ
- Myr - Myr - Myr
Phospho-Akl1
Akl1
Blot: α-GFP
C
Ypk1-3HA
Wildtype
ypk1Δ
ypk2Δ
Myriocin: - + - + - +
Ypk1-3HA
Ypk1
Ypk2
Blot: α-pT662 Ypk1
Blot: α-HA
Red: α-HA
Green: α-pT662 Ypk1
D
Ypk1D242A-3HA
Wildtype
slm1Δ slm2Δ
Myriocin: - + - +
Ypk1D242A-3HA
Ypk1
Ypk2
Blot: α-pT662 Ypk1
Blot: α-HA

Figure 4

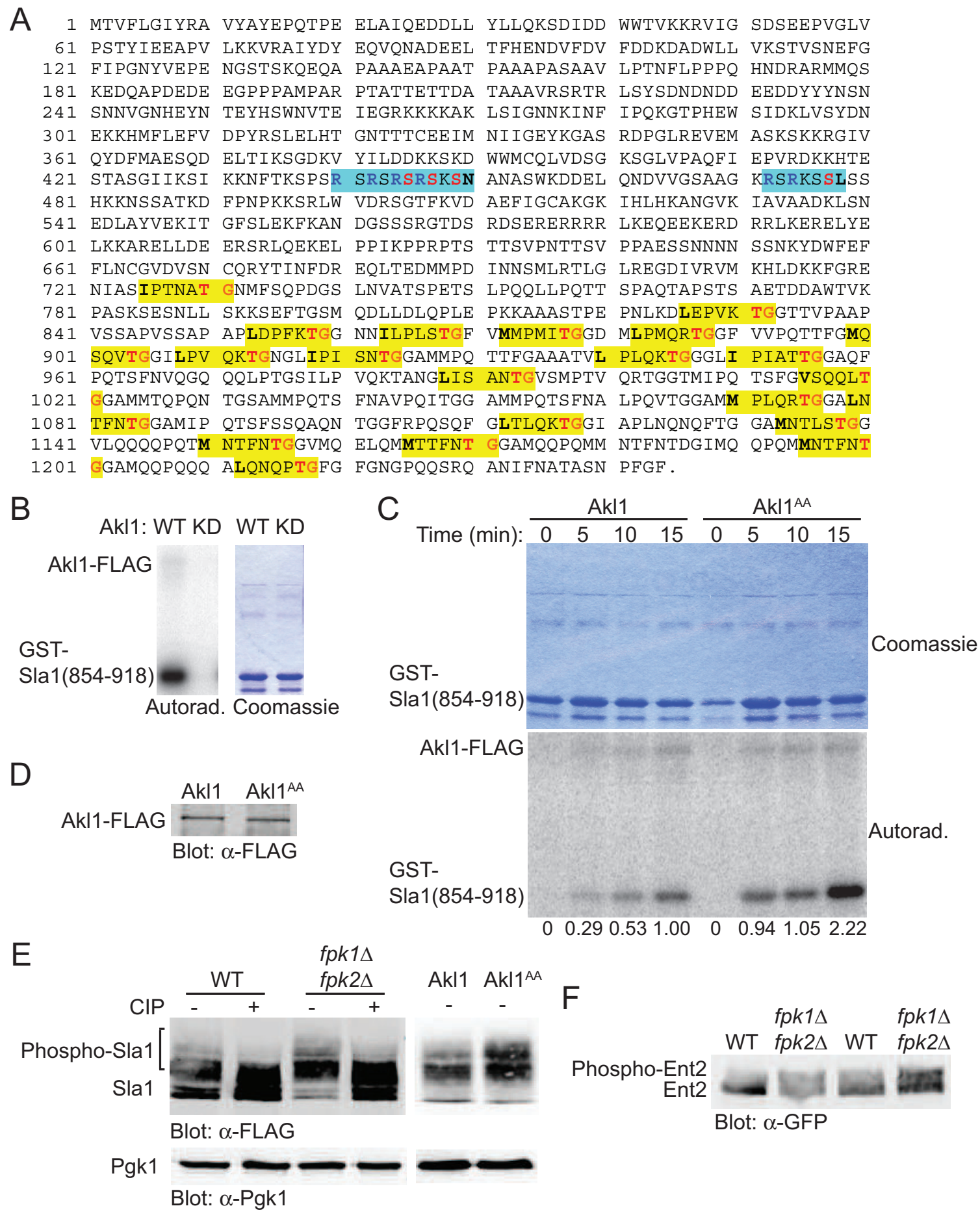
A
1 MTVFLGIYRA VYAYEPQTPE ELAIQEDDLL YLLQKSDIDD WWTVKKRVIG SDSEEPVGLV
61 PSTYIEEAPV LKKVRAIYDY EQVQNADEEL TFHENDVFDV FDDKDADWLL VKSTVSNEFG
121 FIPGNYVEPE NGSTSKQEQA PAAAEAPAAT PAAAPASAAV LPTNFLPPPQ HNDRARMMQS
181 KEDQAPDEDE EGPPPAMPAR PTATTETTDA TAAAVRSRTR LSYSDNDNDD EEDDYYYNSN
241 SNNVGNHEYN TEYHSWNVTE IEGRKKKKAK LSIGNNKINF IPQKGTPHEW SIDKLVSYDN
301 EKKHMFLEFV DPYRSLELHT GNTTTCEEIM NIIGEYKGAS RDPGLREVEM ASKSKKRGIV
361 QYDFMAESQD ELTIKSGDKV YILDDKKSKD WWMCQLVDSG KSGLVPAQFI EPVRDKKHTE
421 STASGIIKSI KKNFTKSPSR SRSRSRSKSN ANASWKDDEL QNDVVGSAAG KRSRKSSLSS
481 HKKNSSATKD FPNPKKSRLW VDRSGTFKVD AEFIGCAKGK IHLHKANGVK IAVAADKLSN
541 EDLAYVEKIT GFSLEKFKAN DGSSSRGTDS RDSERERRRR LKEQEEKERD RRLKERELYE
601 LKKARELLDE ERSRLQEKEL PPIKPPRPTS TTSVPNTTSV PPAESSNNNN SSNKYDWFEF
661 FLNCGVDVSN CQRYTINFDR EQLTEDMMPD INNSMLRTLG LREGDIVRVM KHLDKKFGRE
721 NIASIPTNAT GNMFSQPDGS LNVATSPETS LPQQLLPQTT SPAQTAPSTS AETDDAWTVK
781 PASKSESNLL SKKSEFTGSM QDLLDLQPLE PKKAAASTPE PNLKDLEPVK TGGTTVPAAP
841 VSSAPVSSAP APLDPFKTGG NNILPLSTGF VMMPMITGGD MLPMQRTGGF VVPQTTFGMQ
901 SQVTGGILPV QKTGNGLIPI SNTGGAMMPQ TTFGAAATVL PLQKTGGGLI PIATTGGAQF
961 PQTSFNVQGQ QQLPTGSILP VQKTANGLIS ANTGVSMPTV QRTGGTMIPQ TSFGVSQQLT
1021 GGAMMTQPQN TGSAMMPQTS FNAVPQITGG AMMPQTSFNA LPQVTGGAMM PLQRTGGALN
1081 TFNTGGAMIP QTSFSSQAQN TGGFRPQSQF GLTLQKTGGI APLNQNQFTG GAMNTLSTGG
1141 VLQQQQPQTM NTFNTGGVMQ ELQMMTTFNT GGAMQQPQMM NTFNTDGIMQ QPQMMNTFNT
1201 GGAMQQPQQQ ALQNQPTGFG FGNGPQQSRQ ANIFNATASN PFGF.
B
Akl1: WT KD WT KD
Akl1-FLAG
GST-Sla1(854-918)
Autorad. Coomassie
C
Akl1
Akl1AA
Time (min): 0 5 10 15 0 5 10 15
Coomassie
GST-Sla1(854-918)
Akl1-FLAG
Autorad.
GST-Sla1(854-918)
0 0.29 0.53 1.00 0 0.94 1.05 2.22
D
Akl1 Akl1AA
Akl1-FLAG
Blot: α-FLAG
E
WT
fpk1Δ fpk2Δ
Akl1 Akl1AA
CIP - + - + - -
Phospho-Sla1
Sla1
Blot: α-FLAG
Pgk1
Blot: α-Pgk1
F
WT fpk1Δ fpk2Δ WT fpk1Δ fpk2Δ
Phospho-Ent2
Ent2
Blot: α-GFP

Figure 5

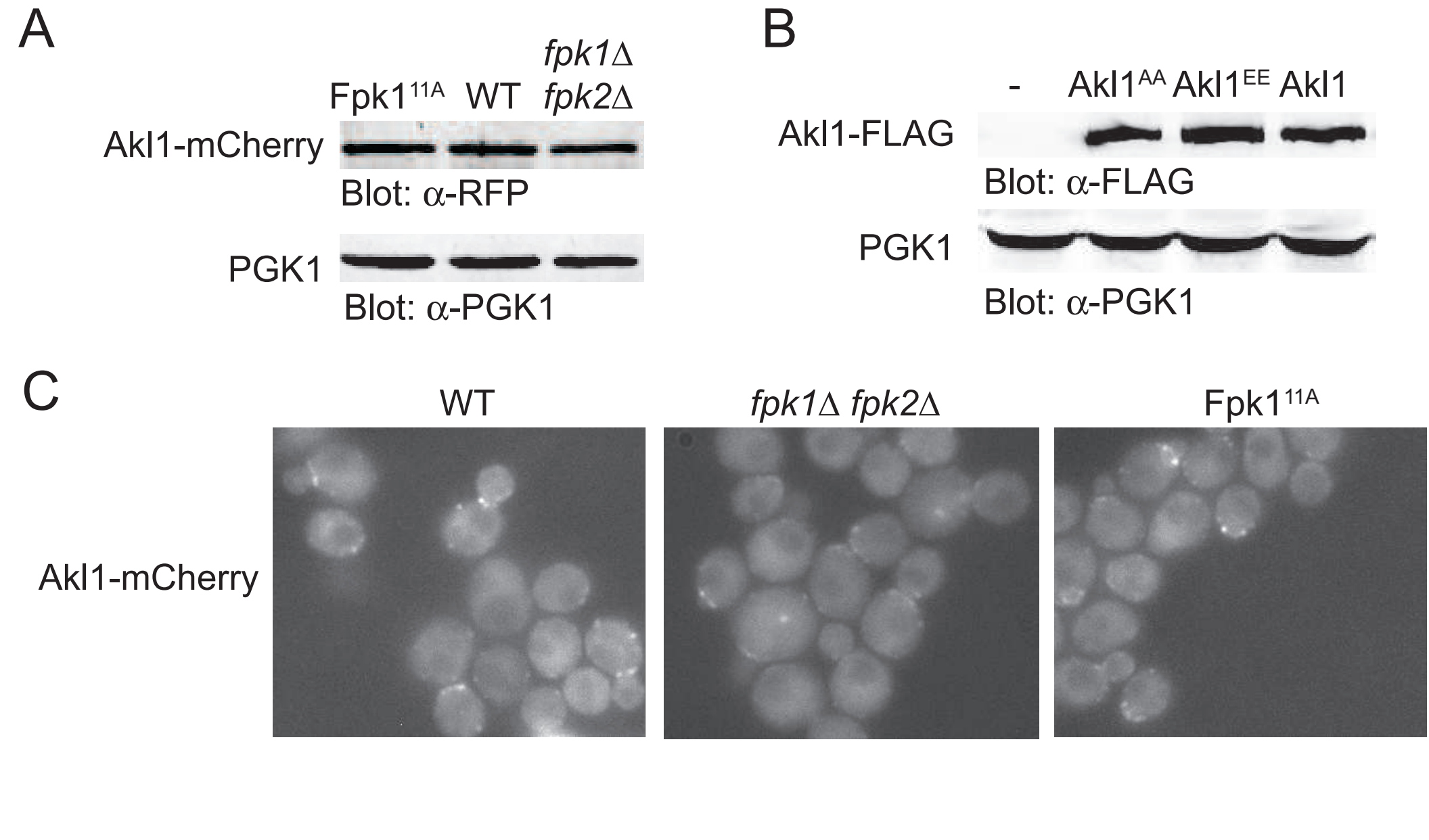
A
Fpk1^11A
WT
fpk1Δ fpk2Δ
Akl1-mCherry
Blot: α-RFP
PGK1
Blot: α-PGK1
B
-
Akl1^AA
Akl1^EE
Akl1
Akl1-FLAG
Blot: α-FLAG
PGK1
Blot: α-PGK1
C
WT
fpk1Δ fpk2Δ
Fpk1^11A
Akl1-mCherry

Figure 6

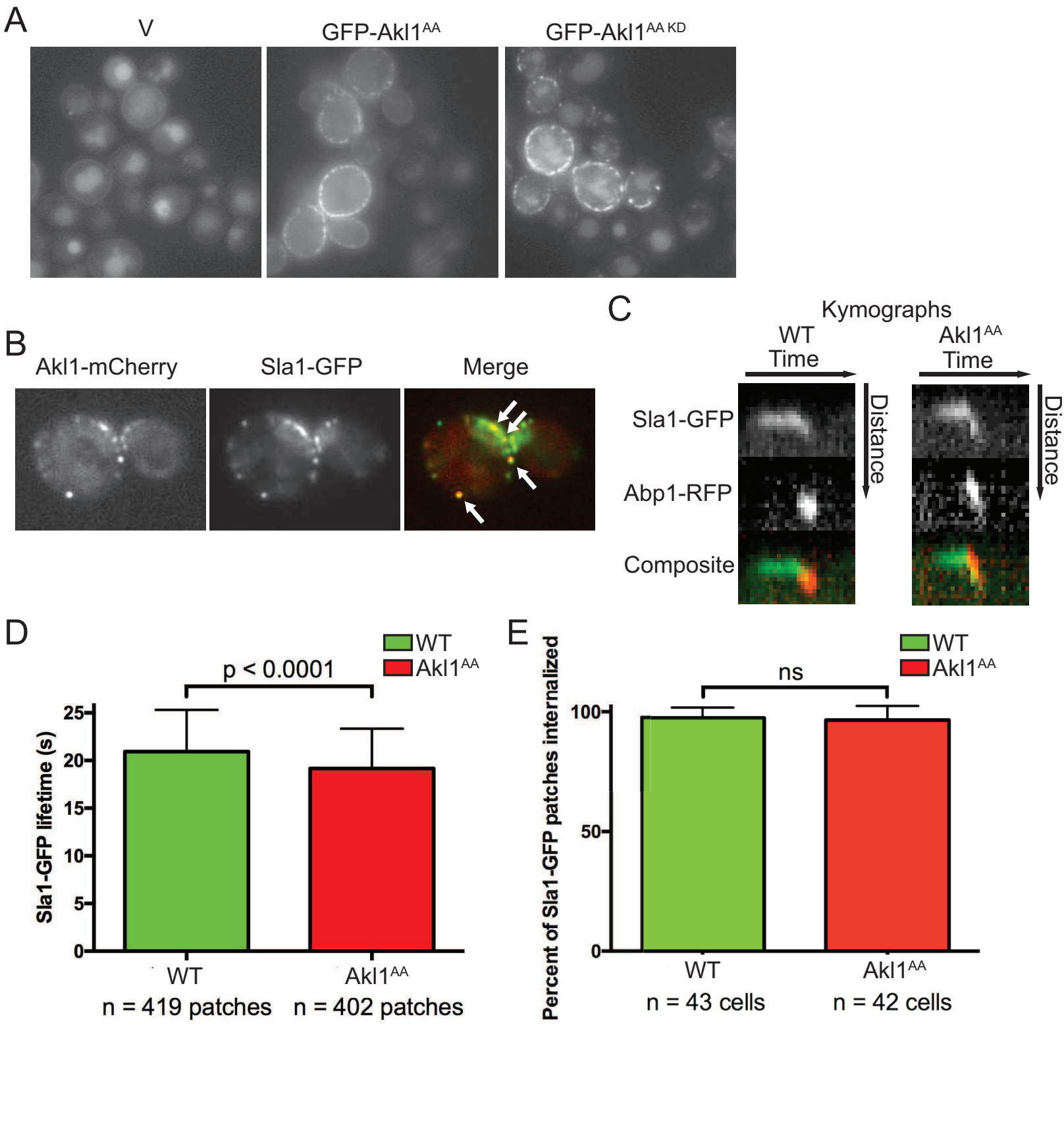
A
V
GFP-Akl1AA
GFP-Akl1AA KD
B
Akl1-mCherry
Sla1-GFP
Merge
C
Kymographs
WT
Time
Akl1AA
Time
Sla1-GFP
Abp1-RFP
Composite
Distance
Distance
D
WT
Akl1AA
p < 0.0001
Sla1-GFP lifetime (s)
25
20
15
10
5
0
WT
Akl1AA
n = 419 patches
n = 402 patches
E
WT
Akl1AA
ns
Percent of Sla1-GFP patches internalized
100
50
0
WT
Akl1AA
n = 43 cells
n = 42 cells

Figure 7

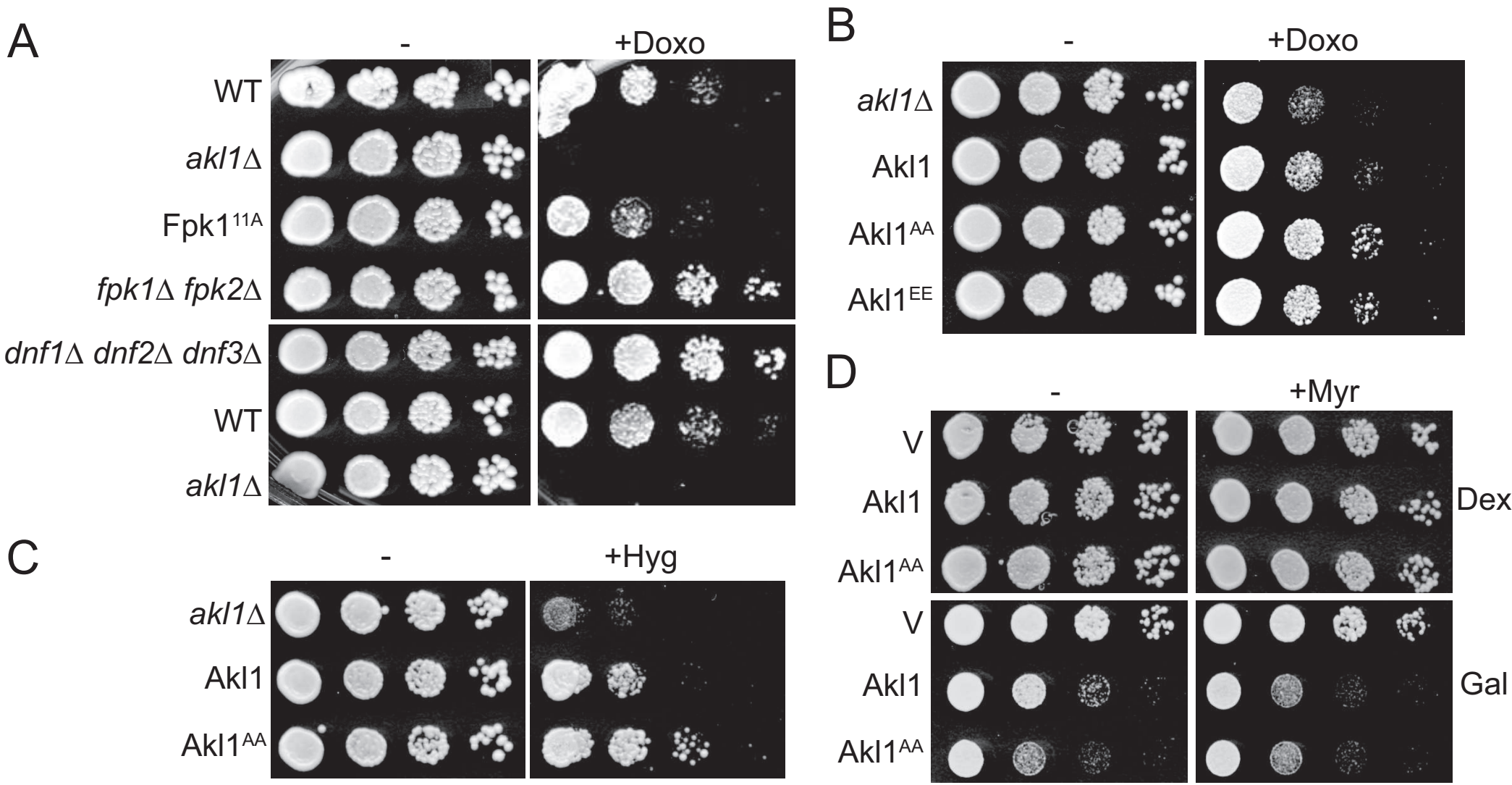
A
-
+Doxo
WT
akl1Δ
Fpk1^11A
fpk1Δ fpk2Δ
dnf1Δ dnf2Δ dnf3Δ
WT
akl1Δ
B
-
+Doxo
akl1Δ
Akl1
Akl1^AA
Akl1^EE
C
-
+Hyg
akl1Δ
Akl1
Akl1^AA
D
-
+Myr
V
Akl1
Akl1^AA
Dex
V
Akl1
Akl1^AA
Gal

Figure 8

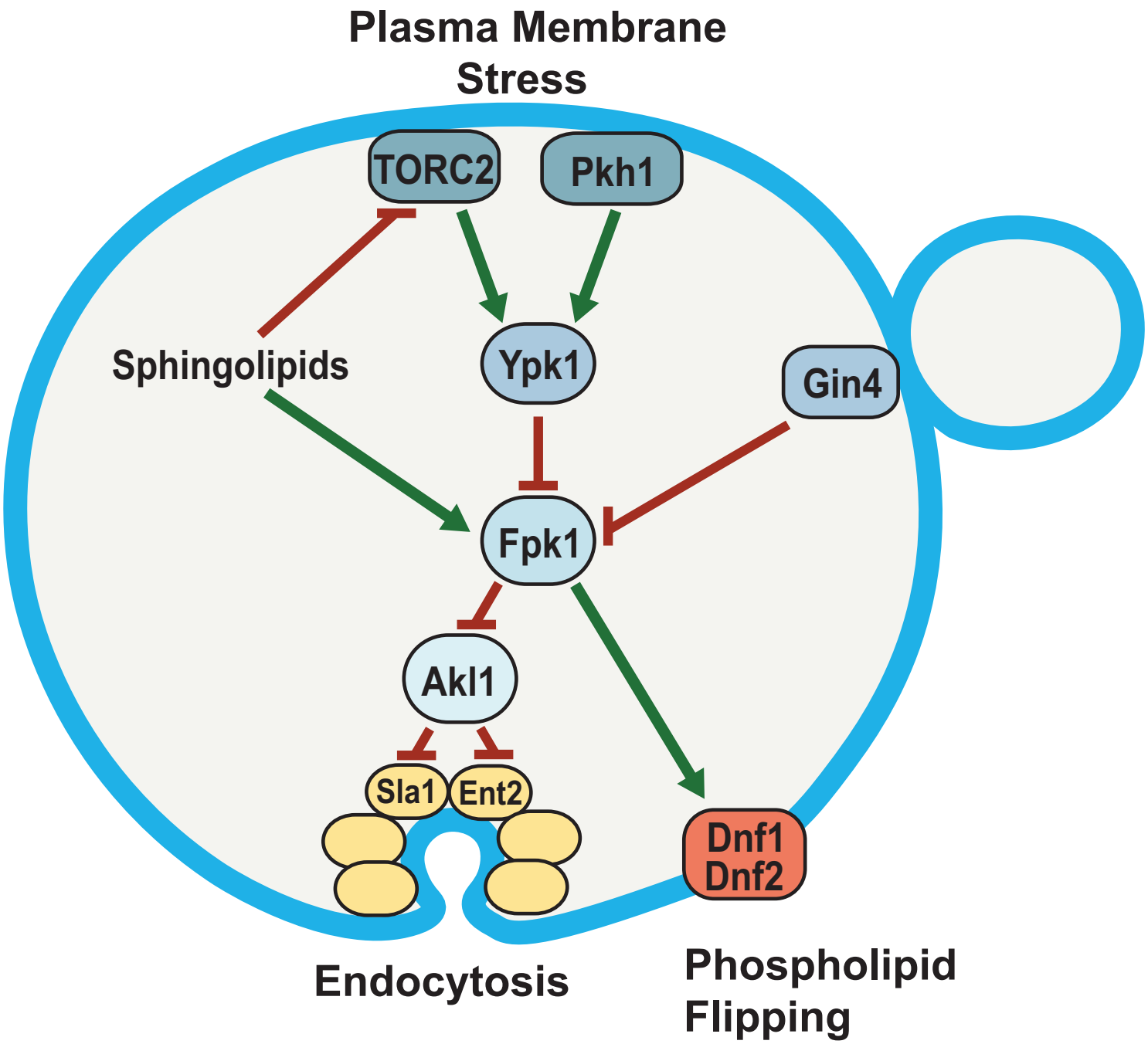
Plasma Membrane
Stress
TORC2
Pkh1
Sphingolipids
Ypk1
Gin4
Fpk1
Akl1
Sla1
Ent2
Dnf1
Dnf2
Endocytosis
Phospholipid
Flipping

Supplemental Figure 1

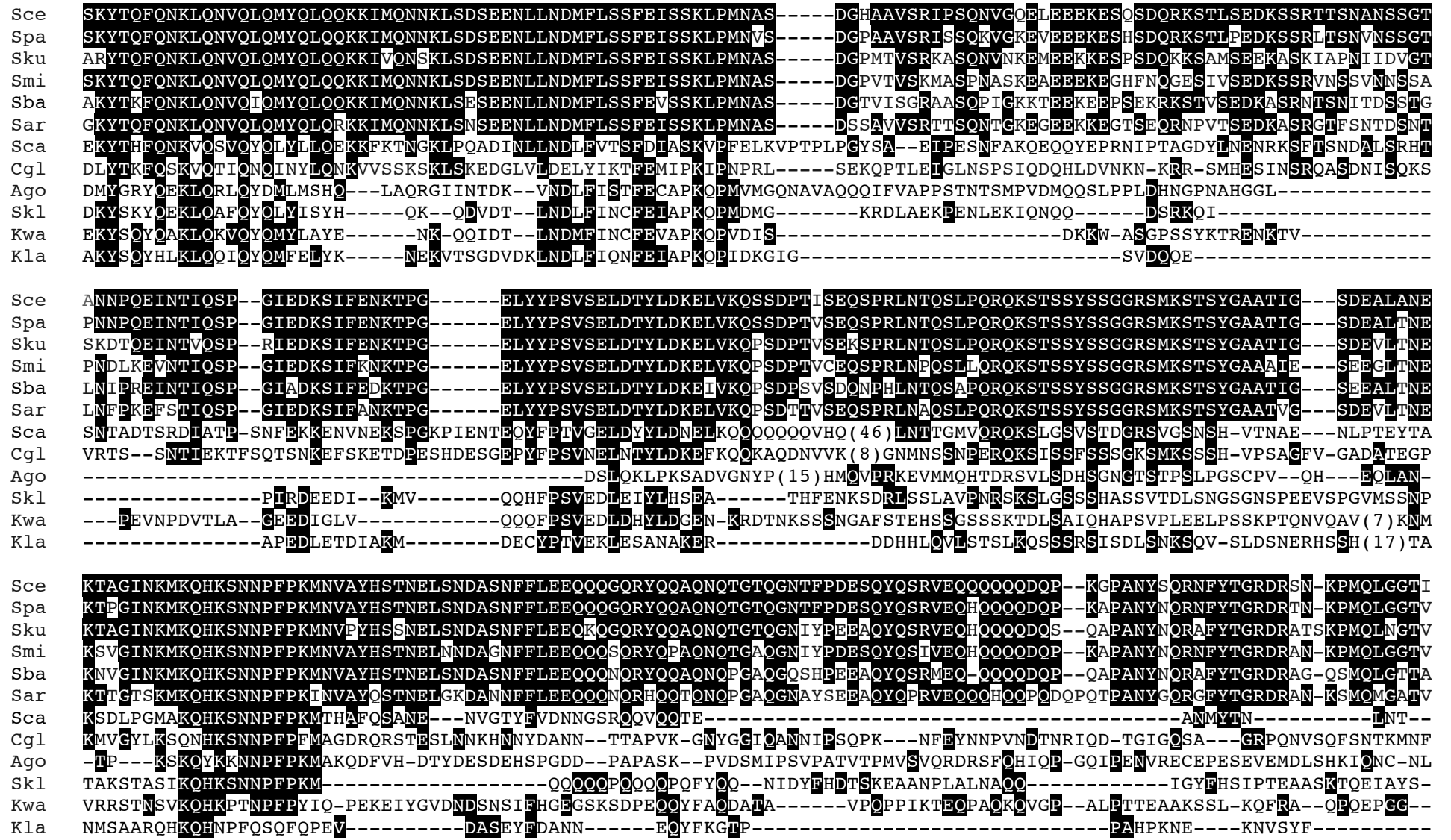
Sce SKYTQFQNKLQNVQLQMYQLQQKKIMQNNKLSDSEENLLNDMFLSSFEISSKLPMNAS-----DGHAAVSRIPSQNVGQELEEEKESQSDQRKSTLSEDKSSRTTSNANSSGT
Spa SKYTQFQNKLQNVQLQMYQLQQKKIMQNNKLSDSEENLLNDMFLSSFEISSKLPMNVS-----DGPAAVSRISSQKVGKEVEEEKESHSDQRKSTLPEDKSSRLTSNVNSSGT
Sku ARYTQFQNKLQNVQLQMYQLQQKKIVQNSKLSDSEENLLNDMFLSSFEISSKLPMNAS-----DGPMTVSRKASQNVNKEMEEKKESPSDQKKSAMSEEKASKIAPNIIDVGT
Smi SKYTQFQNKLQNVQLQMYQLQQKKIMQNNKLSDSEENLLNDMFLSSFEISSKLPMNAS-----DGPVTVSKMASPNASKEAEEEKEGHFNQGESIVSEDKSSRVNSSVNNSSA
Sba AKYTKFQNKLQNVQIQMYQLQQKKIMQNNKLSESEENLLNDMFLSSFEVSSKLPMNAS-----DGTVISGRAASQPIGKKTEEKEEPSEKRKSTVSEDKASRNTSNITDSSTG
Sar GKYTQFQNKLQNVQLQMYQLQRKKIMQNNKLSNSEENLLNDMFLSSFEISSKLPMNAS-----DSSAVVSRTTSQNTGKEGEEKKEGTSEQRNPVTSEDKASRGTFSNTDSNT
Sca EKYTHFQNKVQSVQYQLYLLQEKKFKTNGKLPQADINLLNDLFVTSFDIASKVPFELKVPTPLPGYSA--EIPESNFAKQEQQYEPRNIPTAGDYLNENRKSFTSNDALSRHT
Cgl DLYTKFQSKVQTIQNQINYLQNKVVSSKSKLSKEDGLVLDELYIKTFEMIPKIPNPRL-----SEKQPTLEIGLNSPSIQDQHLDVNKN-KRR-SMHESINSRQASDNISQKS
Ago DMYGRYQEKLQRLQYDMLMSHQ---LAQRGIINTDK--VNDLFISTFECAPKQPMVMGQNAVAQQQIFVAPPSTNTSMPVDMQQSLPPLDHNGPNAHGGL----------
Skl DKYSKYQEKLQAFQYQLYISYH-----QK--QDVDT--LNDLFINCFEIAPKQPMDMG-------KRDLAEKPENLEKIQNQQ------DSRKQI----------
Kwa EKYSQYQAKLQKVQYQMYLAYE------NK-QQIDT--LNDMFINCFEVAPKQPVDIS----------DKKW-ASGPSSYKTRENKTV----------
Kla AKYSQYHLKLQQIQYQMFELYK-----NEKVTSGDVDKLNDLFIQNFEIAPKQPIDKGIG----------SVDQQE----------
Sce ANNPQEINTIQSP--GIEDKSIFENKTPG------ELYYPSVSELDTYLDKELVKQSSDPTISEQSPRLNTQSLPQRQKSTSSYSSGGRSMKSTSYGAATIG---SDEALANE
Spa PNNPQEINTIQSP--GIEDKSIFENKTPG------ELYYPSVSELDTYLDKELVKQSSDPTVSEQSPRLNTQSLPQRQKSTSSYSSGGRSMKSTSYGAATIG---SDEALTNE
Sku SKDTQEINTVQSP--RIEDKSIFENKTPG------ELYYPSVSELDTYLDKELVKQPSDPTVSEKSPRLNTQSLPQRQKSTSSYSSGGRSMKSTSYGAATIG---SDEVLTNE
Smi PNDLKEVNTIQSP--GIEDKSIFKNKTPG------ELYYPSVSELDTYLDKELVKQPSDPTVCEQSPRLNPQSLLQRQKSTSSYSSGGRSMKSTSYGAAAIE---SEEGLTNE
Sba LNIPREINTIQSP--GIADKSIFEDKTPG------ELYYPSVSELDTYLDKEIVKQPSDPSVSDQNPHLNTQSAPQRQKSTSSYSSGGRSMKSTSYGAATIG---SEEALTNE
Sar LNFPKEFSTIQSP--GIEDKSIFANKTPG------ELYYPSVSELDTYLDKELVKQPSDTTVSEQSPRLNAQSLPQRQKSTSSYSSGGRSMKSTSYGAATVG---SDEVLTNE
Sca SNTADTSRDIATP-SNFEKKENVNEKSPGKPIENTEQYFPTVGELDYYLDNELKQQQQQQQVHQ(46)LNTTGMVQRQKSLGSVSTDGRSVGSNSH-VTNAE---NLPTEYTA
Cgl VRTS--SNTIEKTFSQTSNKEFSKETDPESHDESGEPYFPSVNELNTYLDKEFKQQKAQDNVVK(8)GNMNSSNPERQKSISSFSSSGKSMKSSSH-VPSAGFV-GADATEGP
Ago ----------DSLQKLPKSADVGNYP(15)HMQVPRKEVMMQHTDRSVLSDHSGNGTSTPSLPGSCPV--QH---EQLAN-
Skl ----------PIRDEEDI--KMV-------QQHFPSVEDLEIYLHSEA------THFENKSDRLSSLAVPNRSKSLGSSSHASSVTDLSNGSGNSPEEVSPGVMSSNP
Kwa ---PEVNPDVTLA--GEEDIGLV----------QQQFPSVEDLDHYLDGEN-KRDTNKSSSNGAFSTEHSSGSSSKTDLSAIQHAPSVPLEELPSSKPTQNVQAV(7)KNM
Kla ----------APEDLETDIAKM--------DECYPTVEKLESANAKER----------DDHHLQVLSTSLKQSSSRSISDLSNKSQV-SLDSNERHSSH(17)TA
Sce KTAGINKMKQHKSNNPFPKMNVAYHSTNELSNDASNFFLEEQQQGQRYQQAQNQTGTQGNTFPDESQYQSRVEQQQQQQDQP--KGPANYSQRNFYTGRDRSN-KPMQLGGTI
Spa KTPGINKMKQHKSNNPFPKMNVAYHSTNELSNDASNFFLEEQQQGQRYQQAQNQTGTQGNTFPDESQYQSRVEQHQQQQDQP--KAPANYNQRNFYTGRDRTN-KPMQLGGTV
Sku KTAGINKMKQHKSNNPFPKMNVPYHSSNELSNDASNFFLEEQKQGQRYQQAQNQTGTQGNIYPEEAQYQSRVEQHQQQQDQS--QAPANYNQRAFYTGRDRATSKPMQLNGTV
Smi KSVGINKMKQHKSNNPFPKMNVAYHSTNELNNDAGNFFLEEQQQSQRYQPAQNQTGAQGNIYPDESQYQSIVEQHQQQQDQP--KAPANYNQRNFYTGRDRAN-KPMQLGGTV
Sba KNVGINKMKQHKSNNPFPKMNVAYHSTNELSNDASNFFLEEQQQNQRYQQAQNQPGAQGQSHPEEAQYQSRMEQ-QQQQDQP--QAPANYNQRAFYTGRDRAG-QSMQLGTTA
Sar KTTGTSKMKQHKSNNPFPKINVAYQSTNELGKDANNFFLEEQQQNQRHQQTQNQPGAQGNAYSEEAQYQPRVEQQQHQQPQDQPQTPANYGQRGFYTGRDRAN-KSMQMGATV
Sca KSDLPGMAKQHKSNNPFPKMTHAFQSANE---NVGTYFVDNNGSRQQVQQTE----------ANMYTN----------LNT--
Cgl KMVGYLKSQNHKSNNPFPFMAGDRQRSTESLNNKHNNYDANN--TTAPVK-GNYGGIQANNIPSQPK---NFEYNNPVNDTNRIQD-TGIGQSA---GRPQNVSQFSNTKMNF
Ago -TP---KSKQYKKNNPFPKMAKQDFVH-DTYDESDEHSPGDD--PAPASK--PVDSMIPSVPATVTPMVSVQRDRSFQHIQP-GQIPENVRECEPESEVEMDLSHKIQNC-NL
Skl TAKSTASIKQHKSNNPFPKM----------QQQQQPQQQQPQFYQQ--NIDYFHDTSKEAANPLALNAQQ----------IGYFHSIPTEAASKTQEIAYS-
Kwa VRRSTNSVKQHKPTNPFPYIQ-PEKEIYGVDNDSNSIFHGEGSKSDPEQQYFAQDATA------VPQPPIKTEQPAQKQVGP--ALPTTEAAKSSL-KQFRA--QPQEPGG--
Kla NMSAARQHKQHNPFQSQFQPEV----------DASEYFDANN------EQYFKGTP----------PAHPKNE----KNVSYF----------

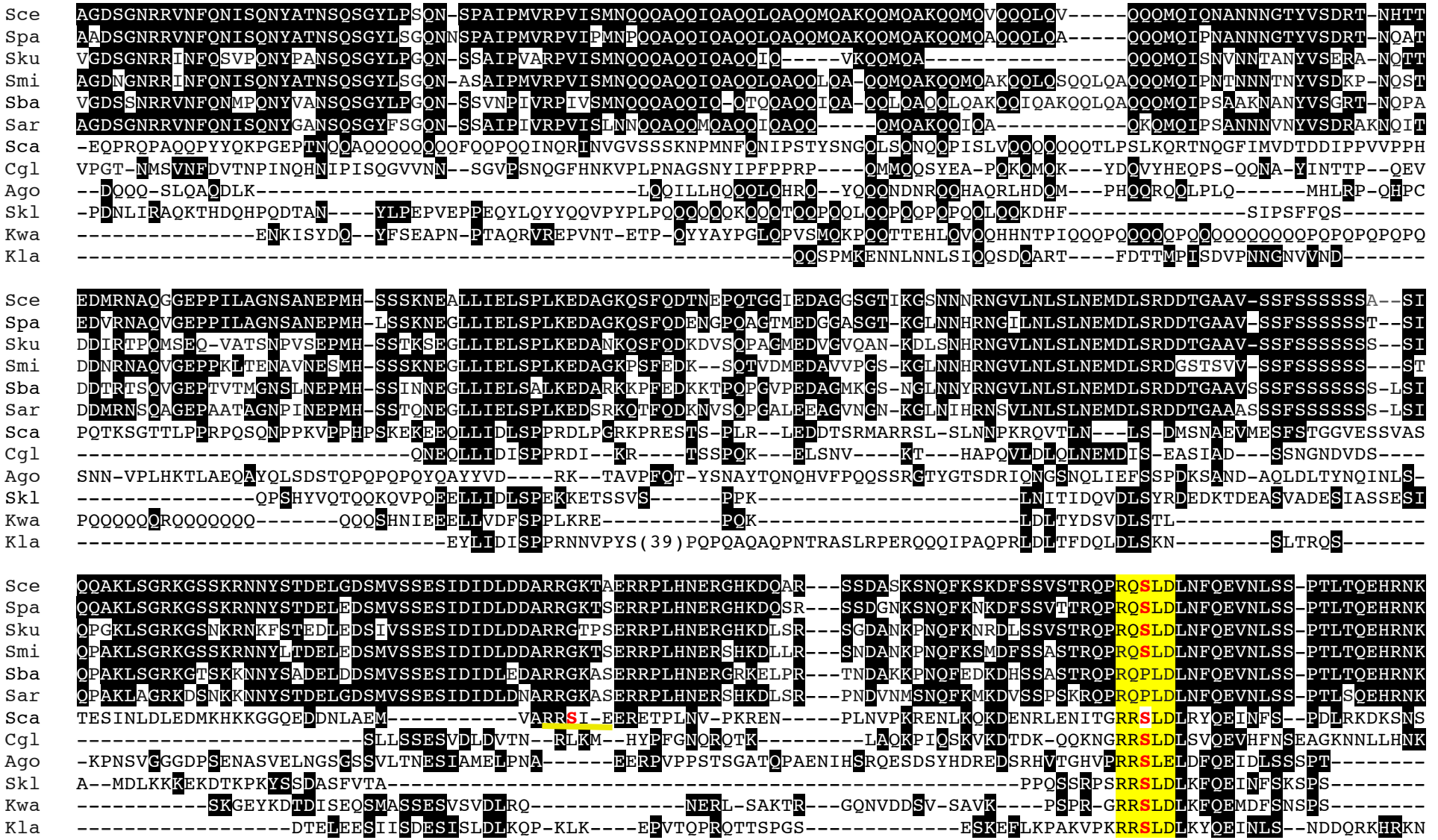
Sce
Spa
Sku
Smi
Sba
Sar
Sca
Cgl
Ago
Skl
Kwa
Kla

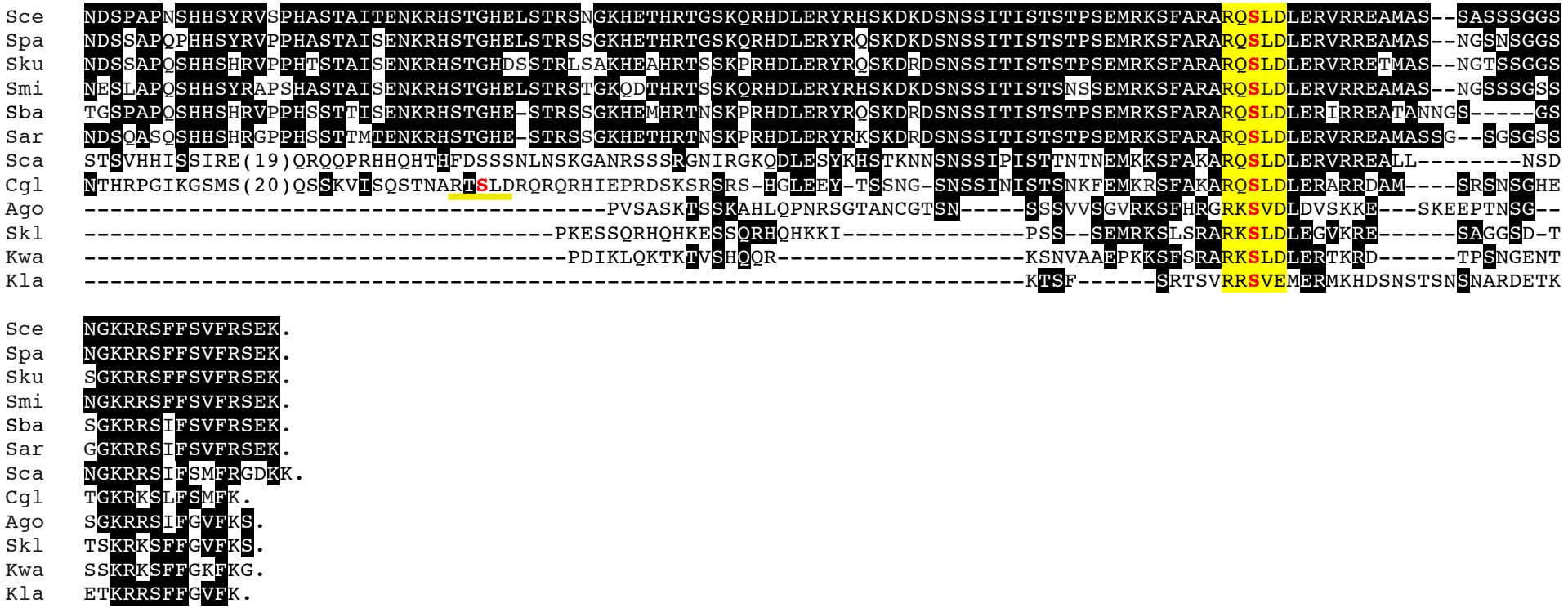

Figure S1. Comparison of Alk1 orthologs from twelve yeast species. The amino acid sequence of *Saccharomyces cerevisiae* Akl1 (*top line*) was aligned with the primary structures of the Alk1 orthologs from eleven other yeast species, including the *sensu stricto* group, *Saccharomyces paradoxus* (Spa), *Saccharomyces kudriavzevii* (Sku), *Saccharomyces mikatae* (Smi), *Saccharomyces bayanus* (Sba), and *Saccharomyces arboricola* (Sar), as well as more divergent species, *Saccharomyces castellii* (Sca), *Candida glabrata* (Cgl), *Ashbya gossypii* (Ago), *Saccharomyces kluyveri* (Skl), *Kluveromyces waltii* (Kwa), and *Kluveromyces lactis* (Kla). As a means to emphasize their degree of relatedness to *S. cerevisiae* Akl1, only identities between the indicated ortholog and *S. cerevisiae* Akl1 are indicated (*white letters on black boxes*). Gaps (*hyphens*), as well as the positions of insertions of the indicated length (*in parentheses*), introduced to maximize the alignment in certain regions are also indicated. Period (.) indicates the end of the open-reading-frame. Matches to the consensus Fpk1 phospho-acceptor site motif (-**R**-x-**S**-**L/V/I**-**D/E**-) (*yellow boxes with phosphorylation site in bold red*); additional site in, respectively, Sca and Clg (*yellow underline*). The sources of the sequences shown were: Sce, strain S288C from the Saccharomyces Genome Datbase (http://www.yeastgenome.org/locus/S000000263/protein); Spa, strain CBS432 derived from the data of Liti *et al.* (2009) and Bergström *et al.* (2014); Sku, Smi, Sba, Sca and Skl as reported by Cliften *et al.* (2003) and Kellis *et al.* (2003); Sar from GenBank entry EJS44833.1; and, Cgl, Ago, Kwa and Kla from the Fungal Orthogroups database at the Broad Institute (https://portals.broadinstitute.org/cgi-bin/regev/orthogroups/show_orthogroup.cgi?orf=YBR059C).

SUPPLEMENTAL REFERENCES

Bergström A, Simpson JT, Salinas F, Barré B, Parts L, Zia A, Nguyen Ba AN, Moses AM, Louis EJ, Mustonen V, Warringer J, Durbin R, Liti G (2014) A high-definition view of functional genetic variation from natural yeast genomes. *Mol. Biol. Evol*. **31**: 872-888.

Cliften P, Sudarsanam P, Desikan A, Fulton L, Fulton B, Majors J, Waterston R, Cohen BA, Johnston M (2003) Finding functional features in Saccharomyces genomes by phylogenetic footprinting. *Science* **301**: 71-76.

Kellis M, Patterson N, Endrizzi M, Birren B, Lander ES (2003) Sequencing and comparison of yeast species to identify genes and regulatory elements. *Nature* **423**: 241-254.

Liti G, Carter DM, Moses AM, Warringer J, Parts L, James SA, Davey RP, Roberts IN, Burt A, Koufopanou V, Tsai IJ, Bergman CM, Bensasson D, O'Kelly MJ, van Oudenaarden A, Barton DB, Bailes E, Nguyen AN, Jones M, Quail MA, Goodhead I, Sims S, Smith F, Blomberg A, Durbin R, Louis EJ (2009) Population genomics of domestic and wild yeasts. *Nature* **458**: 337-341.